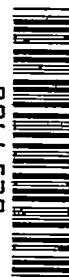


9586

NACA TN 3570

0066539



TECH LIBRARY KAFB, NM

NATIONAL ADVISORY COMMITTEE FOR AERONAUTICS

TECHNICAL NOTE 3570

AN EXPERIMENTAL COMPARISON OF THE LAGRANGIAN AND
EULERIAN CORRELATION COEFFICIENTS IN HOMOGENEOUS
ISOTROPIC TURBULENCE

By William R. Mickelsen

Lewis Flight Propulsion Laboratory
Cleveland, Ohio



Washington
October 1955

AFM 6
TECHNICAL LIBRARY
AFL 201



0066539

NACA TN 3570

TABLE OF CONTENTS

	Page
SUMMARY	1
INTRODUCTION	1
THEORETICAL ANALYSIS	4
The Taylor Theory of Diffusion	4
Solution for the Point Source of Diffusion in a Moving Stream . .	5
Relations Between the Eulerian Correlation Coefficients in Homogeneous Isotropic Turbulence	6
Comparison of the Lagrangian and Eulerian Correlation Coefficients	7
APPARATUS	8
Ducting and Air-Flow Instrumentation	8
Turbulence Instrumentation	9
Helium Injection and Sampling	9
PROCEDURE	9
Mean Stream Conditions	9
Turbulence Measurements	10
Diffusion Measurements	10
RESULTS	11
General Stream Conditions	11
Lateral Turbulence-Intensity Measurements	11
Longitudinal Turbulence-Intensity Measurements	11
Radial Measurements of the Eulerian Correlation Coefficient g .	11
Axial Measurements of the Eulerian Correlation Coefficient f .	12
Turbulent-Spreading-Coefficient Measurements	12
DISCUSSION	13
Homogeneity of the Turbulence Field	13
Isotropy of the Turbulence Field	14
Agreement of the Diffusion Data with the Taylor Theory of Diffusion	15
Comparison of the Shapes of the Lagrangian and Eulerian Corre- lation Coefficients	16
Additional Evaluation of the Proportionality Factor B	17
CONCLUSIONS	17
APPENDIXES	
A - SYMBOLS	19
B - HOT-WIRE ANEMOMETRY	21
Anemometry Equipment	21
Turbulence-Intensity Measurement	21
Correlation-Coefficient Measurement	22
REFERENCES	23

3781

NATIONAL ADVISORY COMMITTEE FOR AERONAUTICS

TECHNICAL NOTE 3570

AN EXPERIMENTAL COMPARISON OF THE LAGRANGIAN AND EULERIAN CORRELATION
COEFFICIENTS IN HOMOGENEOUS ISOTROPIC TURBULENCE

By William R. Mickelsen

SUMMARY

An experimental comparison was made between the Lagrangian and Eulerian correlation coefficients in the homogeneous, isotropic central core of a turbulent pipe flow. The Lagrangian correlation coefficient was characterized by measurements of the turbulent diffusion of helium from a point source. The turbulence intensity and Eulerian correlation coefficients were measured by hot-wire anemometry.

The Lagrangian and Eulerian correlation coefficients had similar shapes related by a linear proportionality between their time and space coordinates. The linearity and the proportionality factor were evaluated over a range of turbulence intensities from 1.8 to 14 feet per second.

The proportionality factor was roughly 0.6 and provides a means for the quantitative solution of practical turbulent-mixing problems from hot-wire-anemometry data or from knowledge of the Eulerian parameters of the turbulence field.

INTRODUCTION

The turbulent mixing of mass and heat is of major importance to the performance of jet-engine combustors. For example, mixing is largely responsible for the preparation of desired fuel-air mixtures and also affects the over-all combustion process. The general objective of this investigation was to find relations between turbulent-mixing theory and experiment which would provide sufficient information for the direct solution of practical mixing problems.

The Taylor theory of diffusion by continuous movements (ref. 1) provides definitions of the turbulent parameters which enter directly into the solution of turbulent-mixing problems. This theory will be discussed in detail in the next section of this report, and it will suffice to say here that the turbulent-mixing parameters are derived

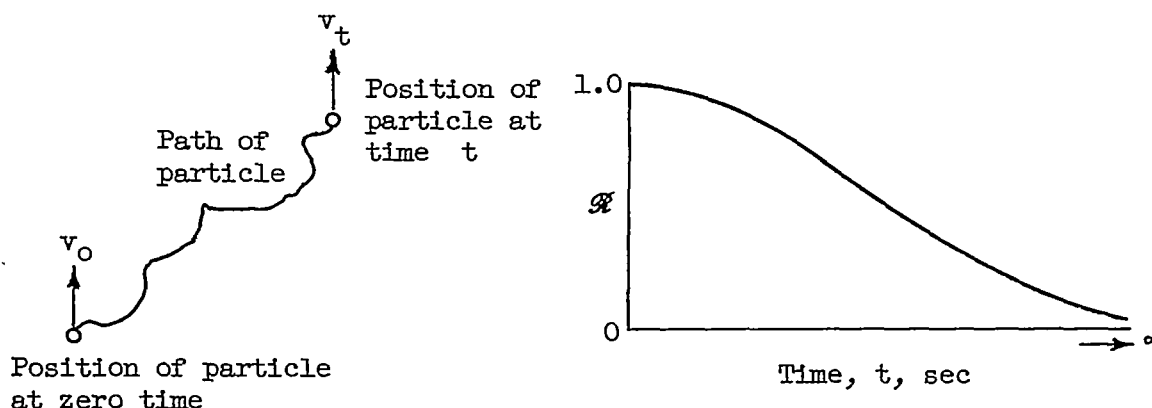
3781

T-1
CV-1

directly from the Lagrangian correlation coefficient \mathcal{R} . This coefficient expresses the degree of correlation between the velocity v_0 of a particle at time t_0 and the velocity v_t of the same particle at a later time t , as shown by the equation

$$\mathcal{R} = \frac{\overline{v_0 v_t}}{v^2} \quad (1)$$

(See appendix A for definitions of symbols.) Equation (1) is written for a homogeneous field of turbulence, and the bar over the velocity products denotes the average of a large number of particle motions. The Lagrangian correlation coefficient \mathcal{R} may be further clarified by the following figures:

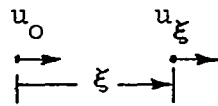


As shown in the right-hand graph, $\mathcal{R} = 1$ at $t = 0$, and \mathcal{R} usually approaches zero as t approaches infinity.

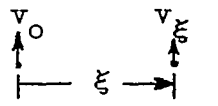
Although the Lagrangian correlation coefficient cannot be measured directly by existing instrumentation, the mixing rate of any particular turbulent field can be determined by measuring the diffusion of mass or heat from a simple source. The Eulerian turbulence parameters of the field can be measured by hot-wire anemometry, or possibly predicted from experience or from the shape of the flow-field boundaries. The direct measurement of the mixing rate is laborious and awkward compared with hot-wire-anemometry techniques; hence, a need exists for knowledge of relations between the Lagrangian and Eulerian parameters of turbulence.

Two important Eulerian measures of a turbulence field are the turbulence intensity $\sqrt{u^2}$ and the double velocity correlation coefficient, a nine-component second-order tensor, which for homogeneous isotropic turbulence can be reduced to two interrelated correlation coefficients f and g , as shown by Kármán and Howarth (ref. 2). The Eulerian correlation

coefficients f and g express the degree of correlation between turbulent-velocity components of different fluid particles at points separated by a distance ξ ;



$$f = \frac{\overline{u_0 u_{\xi}}}{\overline{u^2}} \quad (2)$$



$$g = \frac{\overline{v_0 v_{\xi}}}{\overline{v^2}} \quad (3)$$

where the bars denote time averages. The relation between f and g is shown in the next section of the report. Both f and g become equal to 1.0 at $\xi = 0$, and both usually are asymptotic to zero as ξ approaches infinity, in a manner similar to that of the Lagrangian correlation coefficient \mathcal{A} . Both f and g can be conveniently measured by present-day hot-wire anemometry.

The only work appearing in the literature on the theoretical relation between the Lagrangian and Eulerian correlation coefficients is that of reference 3. The analysis is based on joint-velocity probability distributions and Eulerian correlation coefficients between successive incremental distances but is not yet in a completely usable form.

A number of experimental measurements of the mixing of mass and heat have been made in turbulent fluid streams. In the work of reference 4, hydrogen and carbon dioxide were injected from a simulated point source into the central core of a fully developed turbulent pipe air flow and were found to diffuse at the same rate. The results agreed with Taylor's theory of diffusion in that the turbulent diffusion coefficient was a function of time which increased from zero to an asymptotic value far downstream.

A similar experiment was performed by measuring the turbulent diffusion of a salt solution from a simulated point source in a fully developed turbulent water channel flow (ref. 5). The results, which agreed with those of reference 4, showed the Lagrangian correlation coefficient to be a continuous function of time having the characteristics discussed in a preceding paragraph.

Measurements have also been made of the turbulent diffusion of heat close behind a line source in a grid-generated flowing turbulence field (refs. 6 to 8). The Taylor theory of diffusion predicts that, for very short times subsequent to the start of the diffusion process, the turbulent diffusion coefficient is equal to $\overline{v^2}t$, where $\overline{v^2}$ is the mean square of the turbulent-velocity fluctuations, and t is the residence

3781

CV-1 back

time in the stream. Reference 6 reports work where the turbulent-diffusion coefficient was equal to that predicted by the Taylor theory, while references 7 and 8 give experimental turbulent-diffusion coefficients higher than those predicted theoretically.

The experimental work of references 7 and 9 included determination of the Lagrangian correlation coefficient in fields of decaying isotropic turbulence. These measurements are also in accord with the Taylor description of the Lagrangian correlation coefficient.

The specific objective of the present investigation was to find a relation between the Lagrangian and the Eulerian turbulence parameters, so that quantitative solutions to mixing problems could be obtained from anemometry measurements of the turbulent field. Lagrangian turbulent-mixing parameters were found experimentally by measuring the diffusion of helium from a point source in an air stream. Helium was used as a diffusing material because it could be detected in very low concentrations with existing mass-spectrometry equipment. The low concentrations were desirable since the helium injection flow rates, and hence the helium injector, could be kept small. In this way, the effect of the injector vortex wake on the diffusion process was minimized. In addition, the low concentrations of helium had a negligible effect on the fluid properties of the stream. The Eulerian correlation coefficients were measured with constant-temperature-anemometry equipment. The experiment was performed in the approximately homogeneous, isotropic central core of fully developed turbulent pipe flow.

The investigation was carried out at the NACA Lewis Flight Propulsion Laboratory as a part of the combustion research program.

THEORETICAL ANALYSIS

Defining the turbulent mixing downstream from a point source in terms of the Lagrangian correlation coefficient provides a comparison between the Lagrangian and Eulerian correlation coefficients. This section shows the derivation of this Lagrangian-mixing relation and also includes Eulerian relations pertinent to the condition of isotropy and to the Lagrangian-Eulerian comparison.

The Taylor Theory of Diffusion

Taylor shows in reference 1 that the mean displacement of fluid particles in a turbulent field is related to the Lagrangian correlation coefficient

$$\frac{1}{2} \frac{\overline{dy^2}}{dt} = \overline{v^2} \int_0^t \alpha \, dt \quad (4)$$

where $\overline{Y^2}$ is the mean square displacement of a group of many particles. Reference 10 points out that by analogy to Brownian movement

$$D = \frac{1}{2} \frac{d\overline{Y^2}}{dt} \quad (5)$$

where D is a turbulent-diffusion coefficient.

As noted in reference 11, experiment (refs. 4 to 9) has indicated that in homogeneous turbulence, the fluid particle displacements Y have a Gaussian probability density. Reference 11 shows that as a consequence of this Gaussian form the diffusion coefficient defined by equation (5) may be used in the Fourier-Poisson diffusion equation

$$\frac{\partial C}{\partial t} = \frac{\partial}{\partial x_i} \left[(D + d) \frac{\partial C}{\partial x_i} \right] \quad (i = 1, 2, 3) \quad (6)$$

where C is the concentration of mass at the coordinates x_i at time t , and d is the molecular-diffusion coefficient.

Solution for the Point Source of Diffusion in a Moving Stream

If the molecular-diffusion coefficient d is constant, as in the present investigation, and if the turbulent field is homogeneous and isotropic, then equation (6) can be written

$$\frac{\partial C}{\partial t} = (D + d) \frac{\partial^2 C}{\partial x_i^2} \quad (i = 1, 2, 3) \quad (7)$$

A new parameter ω may be defined by the relation

$$\omega = \omega_T + \omega_d = \int_0^t (D + d) dt \quad (8)$$

where ω , ω_T , and ω_d are called the total, the turbulent, and the molecular-spreading coefficients, respectively. Through this transformation, equation (7) may be written

$$\frac{\partial C}{\partial \omega} = \frac{\partial^2 C}{\partial x_i^2} \quad (i = 1, 2, 3) \quad (9)$$

The solution to equation (9) for an instantaneous point source released into a stream having a velocity U is given in reference 12 as

$$C = \frac{W}{(4\pi\omega)^{3/2}} e^{-\frac{(x-Ut)^2 + r^2}{4\omega}} \quad (10)$$

Reference 13 notes that the solution for a continuous point source can be obtained by summing the contributions from the infinite number of diffusion centers downstream from the injection point;

$$C = \frac{W}{(4\pi)^{3/2}} \int_0^\infty \frac{1}{\omega^{3/2}} e^{-\frac{(x-Ut)^2 + r^2}{4\omega}} dt \quad (11)$$

An approximate solution for the continuous point source suggested in reference 4 for cases where the diffusion in the x direction is negligible and where $x \gg r$ is

$$C = \frac{W}{4\pi\omega} e^{-\frac{r^2}{4\omega}} \quad (12)$$

The validity of equation (12) was checked in the present investigation by comparing it numerically with a graphical solution of equation (11). The comparison indicated that equations (11) and (12) are practically identical over a range of r sufficient for the evaluation of ω .

Relations Between the Eulerian Correlation Coefficients in

Homogeneous Isotropic Turbulence

For homogeneous, isotropic turbulence, Karman and Howarth (ref. 2) show that the Eulerian double velocity correlation coefficient is a second-order tensor, that is,

$$\begin{vmatrix} f & 0 & 0 \\ 0 & f & 0 \\ 0 & 0 & g \end{vmatrix} \quad (13)$$

where the correlation coefficients f and g (eqs. (2) and (3)) are related through the equation

$$f - g = -\frac{\xi}{2} \frac{df}{d\xi} \quad (14)$$

Another requirement for the condition of isotropy is that

$$\sqrt{u^2} = \sqrt{v^2} = \sqrt{w^2} \quad (15)$$

Equations (14) and (15) provide means for ascertaining the degree of isotropy in the experimental turbulent stream.

Comparison of the Lagrangian and Eulerian Correlation Coefficients

A Lagrangian scale of turbulence \mathcal{L} may be defined by the relation

$$\mathcal{L} = \sqrt{v^2} t^* \quad (16)$$

where t^* is a characteristic time given by

$$t^* = \int_0^\infty \mathcal{R} dt \quad (17)$$

Combining equations (16) and (17) gives

$$\mathcal{L} = \sqrt{v^2} \int_0^\infty \mathcal{R} dt \quad (18)$$

In an analogous manner, an Eulerian scale can be defined by

$$L_F = \int_0^\infty f d\xi \quad (19)$$

For a homogeneous field of turbulence, the Lagrangian and Eulerian scales are proportional;

$$L_F = B \mathcal{L} \quad (20)$$

Furthermore, if the Lagrangian and Eulerian correlation coefficients have the same functional forms, then a basis for their comparison can be expressed by

$$f(\xi) = \mathcal{R} \left(\frac{\xi}{B \sqrt{v^2}} \right) \quad (21)$$

where B is a numerical factor of proportionality. Introduction of equations (20) and (21) into (19) yields equation (18), as consistency requires.

The Lagrangian data taken in the present investigation consisted of the spreading coefficient ω which, when corrected for the molecular spreading through equation (8), was reduced to the turbulent-spreading coefficient ω_T . Combination of equations (4), (5), and (8) results in the following expression for ω_T :

$$\omega_T = \overline{v^2} \int_0^t \int_0^t \mathcal{R} \, dt \, dt \quad (22)$$

Rather than perform a double differentiation of the ω_T data, it was deemed more accurate to perform a double integration of the Eulerian correlation coefficient f by the relation

$$\omega_T = \int_0^\xi \int_0^\xi f \, d\xi \, d\xi \quad (23)$$

By comparison between the ω_T calculated from the anemometry data and the ω_T obtained from the helium-diffusion data, the similarity hypothesis expressed by equation (21) could be investigated.

As shown by the discussion in this section, it is possible to compare the shape characteristics of the Lagrangian and Eulerian correlation coefficients by a combination of helium-diffusion and hot-wire-anemometry measurements.

APPARATUS

Ducting and Air-Flow Instrumentation

The turbulent field was generated in an 8-inch-diameter duct having an inlet length-to-diameter ratio of 36. As shown in figure 1, room air was drawn into the duct through an inlet contraction nozzle and two screens to promote nearly fully developed pipe turbulence at the helium injector and instrumentation stations. The air flow passed through a critical-flow "exhaust choke" station and then into the laboratory altitude exhaust facility. The air-flow rate was controlled by varying the exhaust area.

The air temperature was measured with a mercury thermometer located outside the duct near the inlet nozzle. Duct static pressures were measured with standard wall taps placed at the instrumentation stations and connected to mercury manometers.

The stream velocity was measured with a standard pitot static probe connected to a micromanometer and with a hot-wire anemometer by using a

vortex-shedding technique described in reference 14. The technique consists of determining the frequency of vortex-shedding from a cylinder with a hot-wire anemometer. The frequency of vortex-shedding n is related to the stream velocity U by the Strouhal number $S' = nd_c/U$, where the Strouhal number S is constant over a large range of Reynolds number based on the cylinder diameter d_c . The hot-wire-anemometry equipment also provided a convenient means for measuring radial and axial stream-velocity profiles.

Turbulence Instrumentation

Hot-wire-anemometry equipment was used to measure the turbulence intensities $\sqrt{u^2}$ and $\sqrt{v^2}$ and the Eulerian correlation coefficients f and g . The hot-wire anemometer was of the constant-temperature type and is described in detail in reference 15. The turbulence intensities were measured with an average-square computer described in reference 15. The correlation coefficients were measured with a magnetic-tape correlation computer. The anemometry equipment and techniques are discussed in appendix B.

Helium Injection and Sampling

Helium was supplied to the simulated point source from a standard 14-liter bottle and a pressure-regulator system. The helium mass flow was metered with calibrated critical-flow orifices and injected into the stream through a simulated point source shown in figure 2. The injector was carefully streamlined to minimize flow disturbances.

The tip of the sampling probe had a 0.040-inch inside diameter and a 0.060-inch outside diameter and could be moved across the duct with a probe actuator. The probe could be positioned at any of the instrumentation stations shown in figure 1. The sample was drawn from the stream with a vacuum pump, metered with calibrated critical-flow orifices, and drawn past a standard leak connected to a helium-leak detector. The leak detector was a mass-spectrometer type and had a linear sensitivity to helium concentration.

PROCEDURE

Mean Stream Conditions

Turbulence and helium-diffusion measurements were made at five stream velocities: 50, 75, 100, 122, and 164 feet per second. The air temperature varied from 70° to 78° F, and the duct static pressure varied

from 26.6 to 29.0 inches of mercury absolute. These variations were caused by day-to-day changes in room temperature and barometric pressure and by ducting pressure drops.

Turbulence Measurements

The turbulence field was investigated in detail by making traverse measurements of the turbulence parameters at each of the instrumentation stations shown in figure 1. The central core of fully developed turbulent pipe flow should approach homogeneity and isotropy. The approach to these conditions was investigated, in addition to the turbulence measurements required for comparison of the Eulerian and Lagrangian correlation coefficients. The data reduction methods for the turbulence measurements are discussed in appendix B.

Diffusion Measurements

Helium-concentration profiles were measured at a series of stations downstream from the injector for each of the five stream velocities. In order to minimize turbulence effects at the injector, most of the diffusion data were taken with the helium injection velocity equal to the stream velocity. With this condition, the helium concentration was too low for satisfactory detection at the stations farthest downstream. To alleviate this condition, injection flow rates were doubled for measurements at these stations. Since the relative concentration C/C_0 at the intermediate stations was unchanged by this procedure, it was concluded that injection at twice stream velocity had no effect on evaluation of the spreading coefficient ω at the stations far downstream.

Since the concentration profiles were three dimensional, it was necessary to locate the peak of the profile carefully. This was done by rotating the sampling probe to change the vertical position of the probe tip and then moving the probe horizontally until the peak was found.

The total-spreading coefficient ω was calculated from the slope of a straight line faired through each set of concentration-profile data, where the data were plotted as $\log (C/C_0)$ against r^2 . The molecular-spreading coefficient ω_d was calculated from the relation

$$\omega_d = td \quad (24)$$

where the molecular-diffusion coefficient d was calculated from the theoretical relations given in reference 16. The turbulent-spreading coefficient ω_T was then calculated from equation (8).

RESULTS

General Stream Conditions

Pitot static probe and hot-wire-anemometer measurements showed that in the field of interest, the mean stream velocity had a flat profile in both the axial and radial directions. The slight variations in the temperature (70° to 78° F) and pressure (26.6 to 29.0 in. Hg abs) affected the molecular-diffusion coefficient of helium somewhat, and this effect was included in the evaluation of the turbulent-spreading coefficient.

Lateral Turbulence-Intensity Measurements

The lateral turbulence intensity $\sqrt{v^2}$ was measured throughout the field of interest for each of the stream velocities used. Typical radial and axial profiles of $\sqrt{v^2}$ are shown in figures 3(a) and (b), respectively. The profiles are essentially flat in both directions.

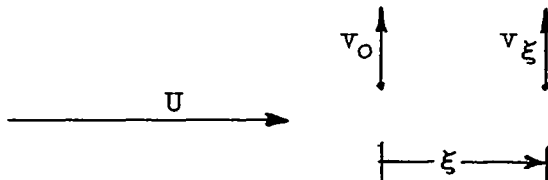
A variation in lateral turbulence intensity with stream velocity was found and is shown in figure 4. This variation might be due to the turbulent field not being fully developed, since the ratio of duct length to diameter was only 36 in contrast to the generally accepted value of 40 to 50.

Longitudinal Turbulence-Intensity Measurements

The longitudinal turbulence intensity $\sqrt{u^2}$ was measured throughout the field of interest and over the range of stream velocities. Typical radial and axial profiles are shown in figures 5(a) and (b), respectively, and are essentially flat.

Radial Measurements of the Eulerian Correlation Coefficient g

Measurements of the Eulerian correlation coefficient g were made throughout the field of interest at each of the stream velocities used. These measurements were made in the radial direction with the X-wire-anemometer probe, so that g was oriented as shown in the following sketch:



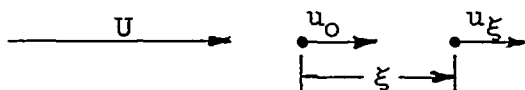
18/81

CV-2 back

A typical series of g measurements along the duct axis at various stations downstream from the helium injector is shown in figure 6(a). The correlation-coefficient curves obtained by fairing lines through the g data as shown in figure 6(a) are summarized in figure 6(b) where a distinct variation in the correlation coefficient with stream velocity can be seen. This may be due to undeveloped turbulent flow, as is a similar trend of $\sqrt{v^2}$.

Axial Measurements of the Eulerian Correlation Coefficient f

The Eulerian correlation coefficient f was measured throughout the field at each of the five stream velocities. These measurements were made in the axial direction with the single-wire-anemometer probe, so that f was oriented as follows:



A typical series of f measurements along the duct axis at various stations downstream from the helium injector is shown in figure 7(a). The solid line in this figure is discussed in the next section. A summary of the measured f correlation coefficients is given in figure 7(b) and shows a variation with stream velocity similar to that of the g correlation coefficients in figure 6(b).

Turbulent-Spreading-Coefficient Measurements

Helium-concentration profiles were measured at a series of stations downstream from the helium injector for each of the five stream velocities. A typical concentration profile is shown in figure 8, where the solid line represents equation (12) fitted to the data by the methods described in the PROCEDURE section. As can be seen from figure 8, the diffusion data follow equation (12) accurately over a range sufficient for evaluation of the total-spreading coefficient ω .

The turbulent-spreading coefficient ω_p was determined from the helium-diffusion data as described in the PROCEDURE section. A summary of the turbulent-spreading-coefficient data is plotted in figure 9 as a function of the distance downstream from the helium injector for each of the five stream velocities. If the turbulence intensities $\sqrt{u^2}/U$, $\sqrt{v^2}/U$, and $\sqrt{w^2}/U$ and the Lagrangian correlation coefficient \mathcal{R} were to remain independent of the stream velocity U , then the Taylor theory of diffusion predicts that all the ω_p data shown in figure 9 should

fall on the same curve when plotted against the distance x . Since both the turbulence-intensity and Eulerian correlation coefficients were dependent on stream velocity, the spread of the ω_T curves in figure 9 is to be expected. An anomalous effect is noted in figure 9 with respect to the ω_T curve for the stream velocity of 122 feet per second. To be consistent with the turbulence measurements and the other four ω_T curves, the ω_T in question should fall below the ω_T for the stream velocity of 164 feet per second, but it does not. This inconsistent result is attributed to experimental error in the diffusion data for the 122-foot-per-second stream velocity.

DISCUSSION

Homogeneity of the Turbulence Field

With the exception of two data points, the turbulent-spreading coefficient ω_T was evaluated from helium concentrations measured within a 2-inch-diameter central core of the pipe flow. This 2-inch core was considered to form the boundary of the turbulence field of interest. The consistency of the values of the turbulence parameters in this field is a measure of the degree of homogeneity of the field. Since the diffusion took place in the radial direction, variations in the lateral turbulence intensity $\sqrt{v^2}$ were deemed important and are listed in the following table for each of the five stream velocities used:

Stream velocity, U , ft/sec	Deviation from the mean value of $\sqrt{v^2}$ in core of interest, percent
50	± 20.6
75	± 8.2
100	± 10.5
122	± 7.2
164	± 14.6

By inspection of data such as those in figure 3(a), some of the deviation shown in this table is attributed to errors in measurement. In

general, the radial profiles of $\sqrt{v^2}$ showed slight trends towards higher values at the outer boundary of the core of interest and exhibited somewhat higher values in the helium-injector wake for locations a few inches downstream from the injector.

The correlation coefficients f and g showed no definite trend in either the radial or lateral direction in the core of interest for

any particular stream velocity. The slight effect noted in the injector wake was attributed to the periodicity of the wake turbulence. This effect decreased the value of the correlation coefficients near $\xi = 0$ and persisted through most of the rest of the correlation curve in the form of ripples superimposed on the generally smooth curve.

Isotropy of the Turbulence Field

Isotropy is defined as the condition wherein the turbulence intensity and correlation tensor are invariant to rotation or to reflection in any plane through the coordinate-system origin (ref. 2). A measure of isotropy is therefore found in the degree of agreement between the values of the turbulence intensity in the rectangular directions. Since only $\sqrt{u^2}$ and $\sqrt{v^2}$ were measured, radial symmetry must be assumed to obtain $\sqrt{v^2} = \sqrt{w^2}$. The agreement between $\sqrt{u^2}$ and $\sqrt{v^2}$ is shown in the following table:

U, ft/sec	$\sqrt{v^2}/U$	$\sqrt{u^2}/U$	$\sqrt{v^2}/\sqrt{u^2}$
50	0.0345	0.0305	1.13
75	.0340	.0310	1.10
123	.0315	.0315	1.00

As discussed in the RESULTS section, the turbulent pipe flow may not have been fully developed because of insufficient inlet length. This might explain the departure from isotropy at the lower stream velocities shown in the preceding table.

As a consequence of isotropy, a relation exists between the Eulerian correlation coefficients f and g (eq. (14)). This relation can be integrated as follows to provide a numerical relation between f and g :

$$f = \frac{2}{\xi^2} \int_0^\xi \xi g \, d\xi \quad (25)$$

The agreement of the measured f and g with equation (25) was found by calculating an f from the measured g by graphical integration. The results of a typical calculation are shown in figure 7(a), where the calculated f is plotted for comparison with the measured f . The agreement between the calculated and measured f correlation coefficients (figs. 10 and 7(b), respectively) was best at the higher stream velocities, which is consistent with the agreement between $\sqrt{u^2}$ and $\sqrt{v^2}$ shown in the preceding table.

In summary, it appears that the condition of isotropy is approached closely, especially at the higher stream velocities. The greater departure from isotropy at the lower stream velocities is of consequence in discussion later in this section.

Agreement of the Diffusion Data with the Taylor Theory of Diffusion

As mentioned in the INTRODUCTION, there are conflicting data about the turbulent-diffusion process for small times (short distances downstream from the diffusion source). By inspection, equation (22) indicates that for small values of t (where $\mathcal{R} \approx 1$) the turbulent-spreading coefficient ω_T should be

$$\omega_T = \frac{1}{2} \overline{v^2} t^2 \quad (26)$$

After correction for hot-wire length, the anemometry measurements of $\overline{v^2}$ in reference 17 were found to accurately predict the turbulent diffusion of heat from a line source by equation (26). In the similar experiments reported in references 7 and 8, the turbulent-spreading coefficients of the heat wake were greater than those predicted from anemometry measurements and equation (26).

The pulse-like nature of the instantaneous temperature measured close behind the line source of heat indicated that the heat wake was a randomly waving sheet having a finite thickness due to molecular diffusion (refs. 7 and 8). Reference 8 suggests that the smallest eddies of the turbulence distort the sheet by rotation and strain so that the spreading coefficient ω_T predicted from the anemometer measurements by equation (26) is less than the ω_T found by temperature-distribution measurements. The criterion for this effect is that only eddies smaller than the molecular wake will contribute to the distortion.

The criterion of microscale small compared with molecular-wake width was evaluated in the present investigation by determining the microscale λ_f from the correlation coefficient r and calculating the molecular-wake width as described in the PROCEDURE section. The microscale λ_f was determined from the definition given in reference 18

$$\frac{1}{\lambda_f^2} = \lim_{\xi \rightarrow 0} \left(\frac{1 - r}{\xi^2} \right) \quad (27)$$

and was found to be approximately 0.015 foot for all stream conditions used in the investigation. The maximum molecular spreading was encountered at $t = 0.0497$ second, where the standard deviation of the

molecular wake $\sqrt{2\omega_d}$ was calculated to be 0.0088 foot. These calculations indicate that the effect described in reference 8 did not occur in the present investigation, since the maximum molecular-wake width was less than the microscale of the turbulence. This conclusion is borne out by a comparison between the ω_T determined from the helium-diffusion data and those calculated from the anemometry measurements and equation (26). This comparison, which shows acceptable agreement between the anemometry data and those measured by diffusion, is tabulated as follows:

Stream velocity, U, ft/sec	Time, t, sec	Spreading coefficient, sq ft		$\frac{1}{2} \overline{v^2} t^2$
		ω_T (from diffusion data)	$\frac{1}{2} \overline{v^2} t^2$ (calculated from anemometry data)	ω_T
50	0.003	0.00001263	0.0000134	1.06
75	.002	.00001134	.000013	1.15
122	.00123	.00001153	.0000111	.96
164	.000937	.00001063	.0000106	1.00

Comparison of the Shapes of the Lagrangian and Eulerian

Correlation Coefficients

As discussed in the THEORETICAL ANALYSIS section, a comparison of the shapes of the Lagrangian and Eulerian correlation coefficients may be made by comparing the spreading coefficient ω_T with an ω_F calculated from the Eulerian correlation coefficient by equation (23). The ω_F calculated from the f correlation coefficients shown in figure 10 are shown in figure 11 as a function of the separation distance ξ . The turbulent-spreading coefficients ω_T measured by helium diffusion and shown in figure 9, are plotted against time t in figure 12 by using the transformation $x = Ut$. In order to determine the validity of equation (21), the separation distance ξ from figure 11 and the time t from figure 12 were cross-plotted (fig. 13) for equal values of ω_F and ω_T . Equation (21) implies a linear relation between the values of ξ and t corresponding to equal values of ω_F and ω_T . The experimental points on figure 13 can be approximated by straight lines, as shown, and equation (21) is thus substantiated.

The factor B in equation (21) was evaluated from the slopes of the faired lines in figure 13 by using values of the lateral turbulence intensity $\sqrt{v^2}$ from figure 4. The factor B is plotted in figure 14 for each of the five stream velocities.

Additional Evaluation of the Proportionality Factor B

As a part of another research program, concentration profiles of acetone vapor were measured downstream from a simulated point source in a 6-inch-diameter duct. Turbulent-spreading coefficients were determined from the acetone-vapor concentration profiles at distances of 20.3 and 24.8 inches downstream from the point of injection.

Longitudinal turbulence intensities $\sqrt{u^2}$ were measured throughout the duct and had approximately flat radial and axial profiles in the field of interest. The turbulence intensity $\sqrt{u^2}$ had a value of 14 feet per second at the stream conditions listed in figure 15.

The correlation coefficient f was also measured at the stream conditions listed above, along the duct axis. These measurements are plotted in figure 15 for a series of downstream stations and show little change with position in the turbulence field.

On the basis of measurements of longitudinal intensity and the f correlation coefficient, values of ω_f were calculated from equation (23) for comparison with the ω_T values obtained from the acetone-vapor diffusion experiment. The cross plot that was made between the two sets of ω_T and ω_f values gave two values of ξ for respective values of t . The (ξ, t) coordinates fell on a straight line having a slope such that the factor B in equation (21) had a value of 0.62. This value of B agrees well with those shown in figure 14.

In summary, the data show that the Lagrangian and Eulerian correlation coefficients have similar shapes connected by an equation such as equation (21) and that the factor of proportionality in this equation is roughly 0.6.

CONCLUSIONS

1. The Lagrangian and Eulerian correlation coefficients in homogeneous, isotropic turbulence have similar shapes.

1825

CV-3

2. The shapes of the Lagrangian and Eulerian correlation coefficients were found to be related by a linear proportionality between their time and space coordinates as shown by the expression

$f(\xi) = \mathcal{R}\left(\frac{\xi}{B \sqrt{v^2}}\right)$. The proportionality factor B is roughly 0.6 throughout a range of turbulence intensities from 1.8 to 14 feet per second.

3. The linear relation between the shapes of the Lagrangian and Eulerian correlation coefficients provides a means for the quantitative solution of practical mixing problems from hot-wire-anemometry data.

Lewis Flight Propulsion Laboratory
National Advisory Committee for Aeronautics
Cleveland, Ohio, August 5, 1955

APPENDIX A

SYMBOLS

The following symbols are used in this report:

B	factor of proportionality in linear relation between shapes of Lagrangian and Eulerian correlation coefficients
C	concentration of diffusing gas or vapor
D	turbulent diffusion coefficient, sq ft/sec
d	molecular diffusion coefficient, sq ft/sec; or cylinder diameter, ft
E	direct current voltage, v
$\sqrt{E^2}$	root-mean-square of alternating voltage, v
f,g	Eulerian double velocity correlation coefficients defined in manner of von Kármán and Howarth
G	electronic amplification factor
K	constant correcting for division of current in Wheatstone bridge
L	Eulerian scale of turbulence
\mathcal{L}	Lagrangian scale of turbulence
n	frequency of vortex-shedding
\mathcal{R}	Lagrangian correlation coefficient
r	radial distance from axis in cylindrical coordinates, ft
S	Strouhal number
t	time, sec
t^*	characteristic time of turbulence, sec
U	stream velocity, ft/sec
u,v,w	turbulent-velocity vectors in x, y, and z directions, respectively, ft/sec

3781

CV-3 back

W	instantaneous point-source strength, lb
w	injection rate, lb/sec
x	distance in axial direction in cylindrical coordinates, in. or ft
Y	fluid particle displacement, ft
α	angular displacement of X-wire array with respect to stream direction, radians
λ	microscale of turbulence, ft
ξ	separation distance between velocity vectors in Eulerian double velocity correlation coefficients, ft
Ω	electrical resistance, ohms
ω	spreading coefficient, sq ft

Subscripts:

b	voltage across Wheatstone bridge
c	cylinder diameter
D	difference between voltages across two Wheatstone bridges
d	molecular
f	pertaining to correlation coefficient f
i	summation convention
o	peak, or no-flow condition
T	turbulent
t	time
ξ	at distance ξ

Barred symbols indicate time average

APPENDIX B

HOT-WIRE ANEMOMETRY

Anemometry Equipment

The hot-wire-anemometry equipment is shown diagrammatically in figure 16. The amplifiers were of the constant-temperature type with a frequency-response flat within 1 decibel from 0 to 100,000 cycles per second. The bridge and amplifier design is discussed in detail in reference 15.

The turbulence intensities were measured with the average-square computer described in reference 15. The computer had a frequency-response-curve flat within 0.3 decibel from 20 to 10,000 cycles per second, a range of 0.02 to 5 volts rms, and a variable-capacitance meter damping circuit. The computer was calibrated with a sine wave, but measured true root-mean-square voltage of complex waves.

The difference amplifier was a standard design with a gain of 1.0 and a flat frequency-response curve within 0.5 decibel between 20 and 20,000 cycles per second. Its function was to obtain the instantaneous difference between the complex voltages from two hot wires.

The magnetic-tape recorder was of the high-speed two-channel type and was used to store the complex voltage signals from the hot-wire anemometers for later analysis.

The correlation computer was used to determine the correlation coefficients from the anemometer voltage signals stored on the magnetic tape. The curve for over-all frequency response of the computer was flat within 0.5 decibel from 25 to 5000 cycles per second. The operation of the computer is described later in this appendix.

The X-wire- and single-wire-anemometer probes for measuring the lateral and longitudinal turbulent velocities, respectively, are shown in figure 17.

Turbulence-Intensity Measurement

The longitudinal turbulence intensity was determined from the equation

$$\frac{\sqrt{u^2}}{U} = \left(\frac{2\Omega_1}{G\Omega_K} \right) \left(\frac{E_b}{E_b^2 - E_{b,q}^2} \right) \sqrt{E^2} \quad (B1)$$

where E_b and $E_{b,0}$ are direct-current voltages measured at flow and no-flow conditions, respectively, and $\sqrt{E^2}$ is the root-mean-square voltage given by the average-square computer. Equation (B1) is based on King's equation and assumes that the natural convection and compressibility effects on the forced convection from the hot wire are negligible.

The lateral turbulence intensity $\sqrt{v^2}$ was determined by the method developed in reference 19 and discussed in reference 20 that relates the lateral velocity fluctuation to the voltage difference between the two hot wires in the X-array through the equation

$$\frac{\sqrt{v^2}}{U} = \frac{\sqrt{E_D^2}}{G \left(\frac{dE_D}{d\alpha} \right)} \quad (B2)$$

Where the root-mean-square voltage $\sqrt{E_D^2}$ is an instantaneous difference voltage read from the average-square computer, and the term $(dE_D)/(d\alpha)$ is the slope of the direct-current difference voltage against the angular position of the X-array with respect to the stream-velocity vector.

Correlation-Coefficient Measurement

The correlation coefficients were measured by a method introduced in reference 21 that inserts an artificial time lag in the turbulence signal from a single anemometer probe. This method has definite operational advantages over the conventional two-probe method, in that only one stationary probe is required and that the anemometer signal may be stored for analysis at convenience.

The correlation computer used in the present investigation, which was designed by D. F. Berg and C. C. Conger of the Lewis laboratory, is shown diagrammatically in figure 18. The magnetic tape supplied to the computer had identical signals on both channels. The computer was equipped with one fixed and one moveable play-back head, so that an adjustable time delay could be introduced between the otherwise identical signals passing through the two channels of the computer. The out-of-phase signals were amplified in their respective channels by amplifiers matched to the high-speed tape recorder. After amplification, the two signals were multiplied instantaneously by an electronic analog multiplier. The analog multiplier was of the modulated carrier-wave type with a special wave form having a frequency of 2 megacycles. The time average value of the product of the two signals was a correlation

coefficient which related the velocities of two different particles at two different times. The time interval between the two velocities was obtained by dividing the separation distance between the two pickup heads by the tape speed. The space interval between the two velocities was obtained by multiplying the time interval by the stream velocity.

Since the turbulence intensity $\sqrt{v^2}/U$ was much less than unity, the lateral displacement of fluid particles during the time lag interval t of the computer was small compared with the longitudinal space interval given by $\xi = Ut$. From this consideration, the correlation coefficient given by the computer should approximate the true Eulerian coefficient. This conclusion is substantiated by measurements reported in reference 22 which show good agreement between correlation coefficients obtained from the computer and a single probe and those obtained by the conventional two-probe method.

REFERENCES

1. Taylor, G. I.: Diffusion by Continuous Movements. Proc. London Math. Soc., vol. 20, 1922, pp. 196-212.
2. von Kármán, Theodore, and Howarth, Leslie: On the Statistical Theory of Isotropic Turbulence. Proc. Roy. Soc. (London), ser. A, vol. 164, Jan. 21, 1938, pp. 192-215.
3. Brier, Glenn W.: The Statistical Theory of Diffusion by Turbulent Eddies. Meteorological Monographs, vol. 1, no. 4, 1951. pp. 15-19.
4. Towle, W. L., and Sherwood, T. K.: Eddy Diffusion - Mass Transfer in the Central Portion of a Turbulent Air Stream. Ind. and Eng. Chem., vol. 31, no. 4, Apr. 1939, pp. 457-462.
5. Kalinske, A. A., and Pien, C. C.: Eddy Diffusion. Ind. and Eng. Chem., vol. 36, no. 3, Mar. 7, 1944, pp. 220-222.
6. Schubauer, G. B.: A Turbulence Indicator Utilizing the Diffusion of Heat. NACA Rep. 524, 1935.
7. Uberoi, Mahinder S., and Corrsin, Stanley: Diffusion of Heat from a Line Source in Isotropic Turbulence. NACA Rep. 1142, 1953. (Supersedes NACA TN 2710.)
8. Townsend, A. A.: The Diffusion Behind a Line Source in Homogeneous Turbulence. Proc. Roy. Soc. (London), ser. A, vol. 224, no. 1159, July 22, 1954, pp. 487-512.

9. Collis, D. C.: The Diffusion Process in Turbulent Flow. Rep. A.55, Council for Sci. and Ind. Res., Div. Aero., Fishermen's Bend, Melbourne (Australia), Dec. 1948.
10. Dryden, Hugh L.: Turbulence and Diffusion. Ind. and Eng. Chem., vol. 31, no. 4, Apr. 1939, pp. 415-425.
11. Batchelor, G. K.: Diffusion in a Field of Homogeneous Turbulence. I. Eulerian Analysis. Australian Jour. Sci. Res., ser. A, vol. 2, 1949, pp. 437-450.
12. Jakob, Max: Heat Transfer. Vol. 1, John Wiley & Sons, Inc., 1949.
13. Frenkiel, F. N.: Turbulent Diffusion: Mean Concentration Distribution in a Flow Field of Homogeneous Turbulence. Vol. III. Advances in Appl. Mech., Academic Press, Inc., 1953, pp. 61-107.
14. Roshko, Anatol: On the Development of Turbulent Wakes from Vortex Streets. NACA TN 2913, 1953.
15. Laurence, James C., and Landes, L. Gene: Auxiliary Equipment and Techniques for Adapting the Constant-Temperature Hot-Wire Anemometer to Specific Problems in Air-Flow Measurements. NACA TN 2843, 1952.
16. Hirschfelder, Joseph O., Curtiss, Charles F., and Bird, R. Byron: Molecular Theory of Gases and Liquids. John Wiley & Sons, Inc., 1954.
17. Dryden, Hugh L., Schubauer, G. B., Mock, W. C., Jr., and Skramstad, H. K.: Measurements of Intensity and Scale of Wind-Tunnel Turbulence and Their Relation to the Critical Reynolds Number of Spheres. NACA Rep. 581, 1937.
18. Taylor, G. I.: Statistical Theory of Turbulence, Pt. I. Proc. Roy. Soc. (London), ser. A, vol. 151, no. A873, Sept. 1935, pp. 421-478.
19. Schubauer, G. B., and Klebanoff, P. S.: Theory and Application of Hot-Wire Instruments in the Investigation of Turbulent Boundary Layers. NACA WR W-86, 1946. (Supersedes NACA ACR 5K27.)
20. Mickelsen, William R., and Laurence, James C.: Measurement and Analysis of Turbulent Flow Containing Periodic Flow Fluctuations. NACA RM E53F19, 1953.

21. Favre, A.: Mesures Statistiques de la Corrélation dans le Temps. Premières applications à l'étude des mouvements turbulents en soufflerie. Pub. No. 67, Office Nat. d'Études et de Recherches Aéro., 1953.
22. Laurence, James C.: Intensity, Scale, and Spectra of Turbulence in Mixing Region of Free Subsonic Jet. NACA TN 3561, 1955.

1872

CV-4

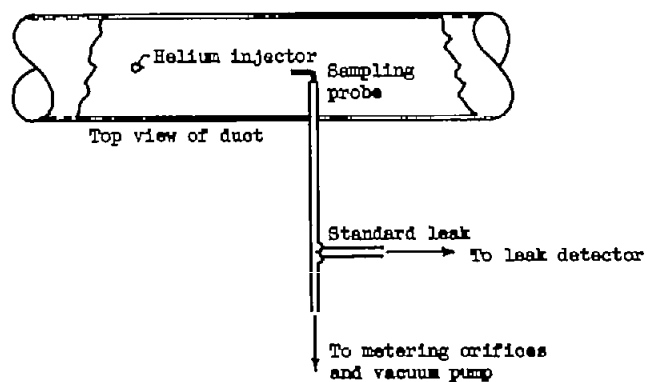
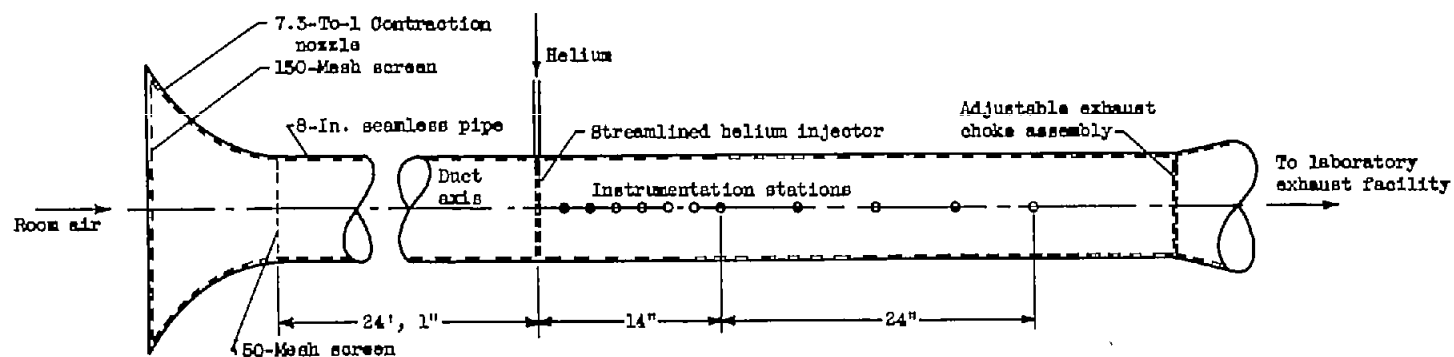


Figure 1. - Air-ducting and helium-sampling apparatus.

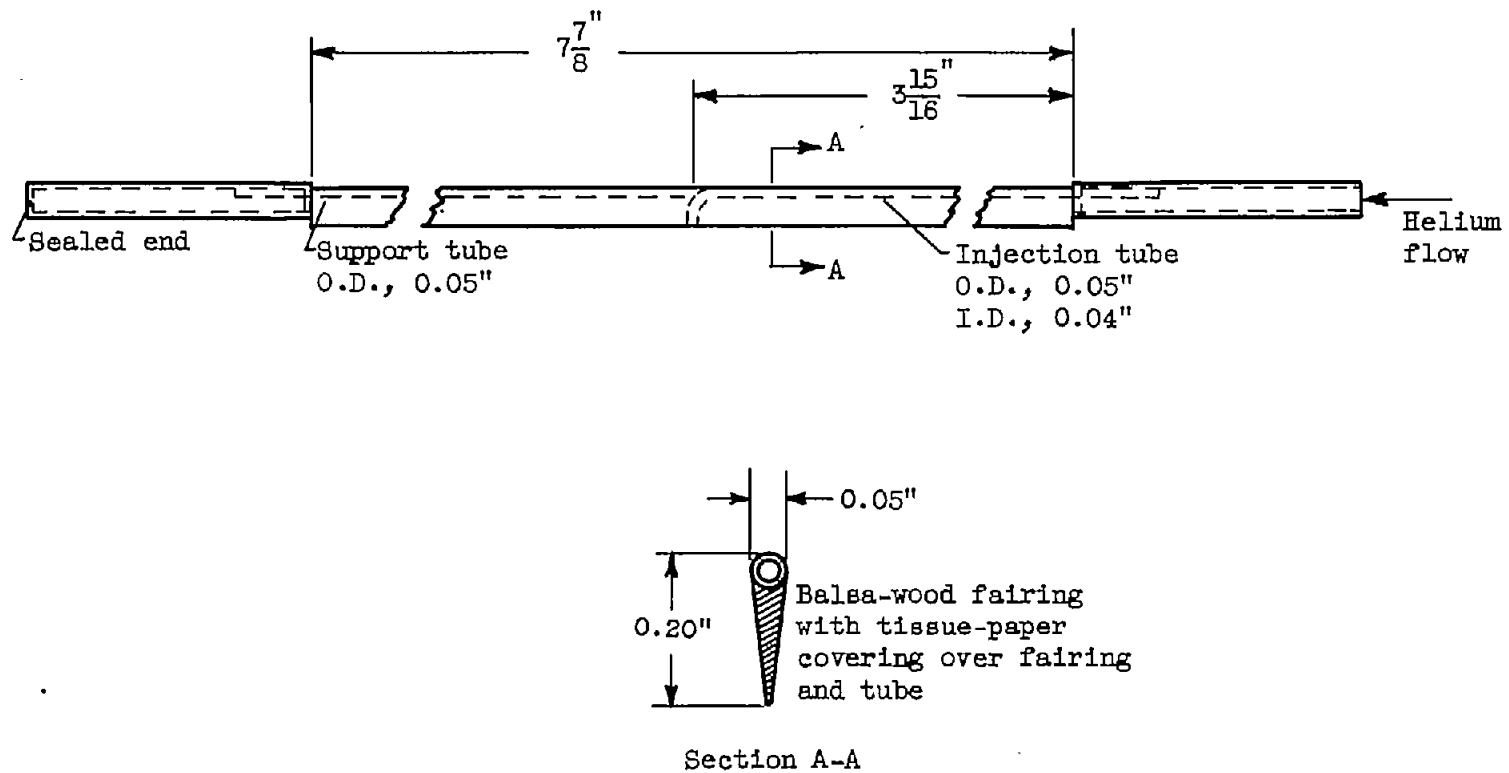
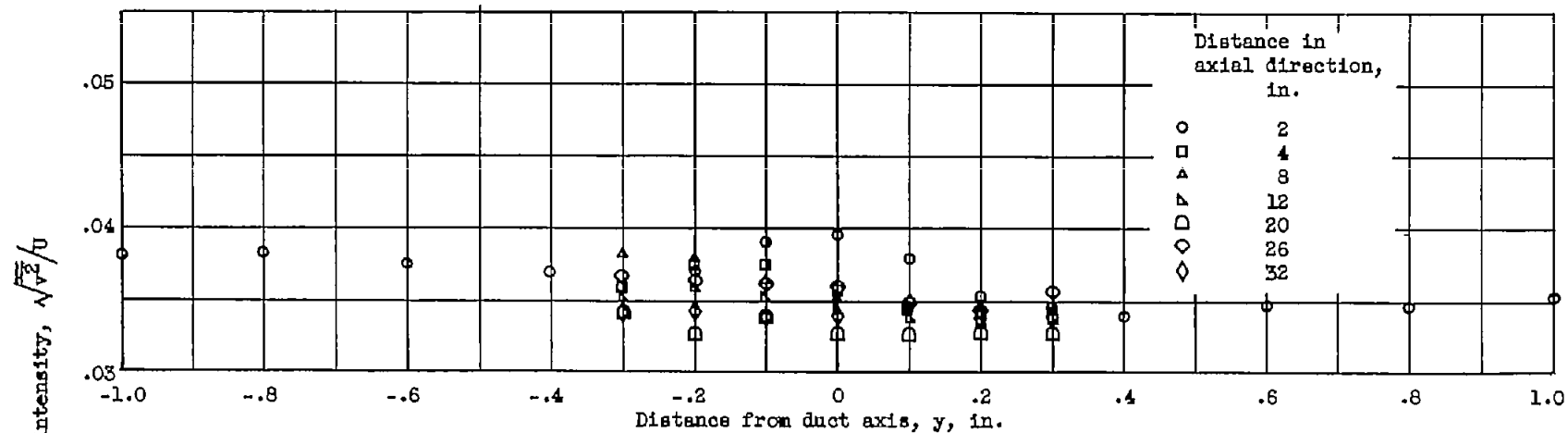
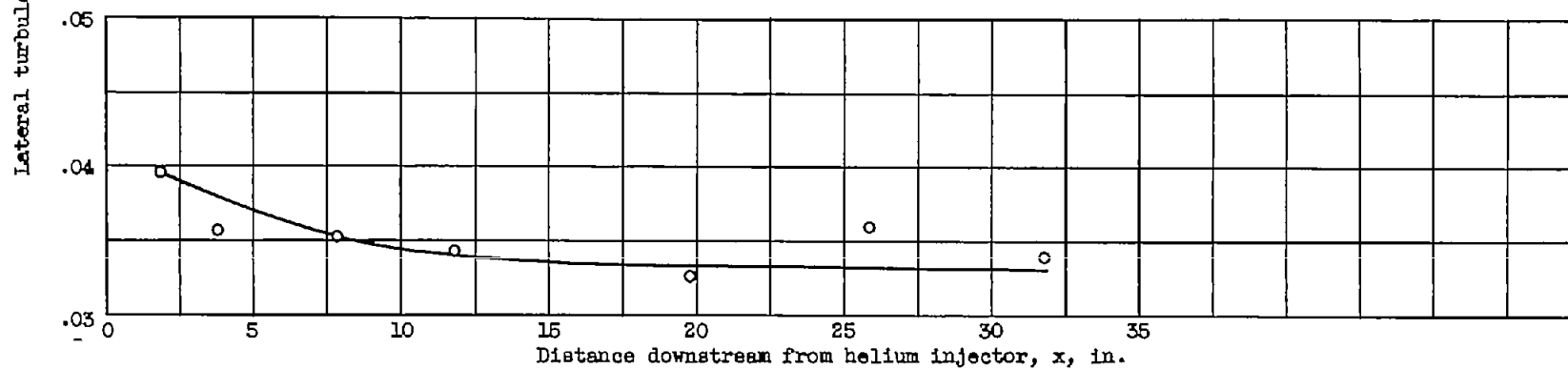


Figure 2. - Helium injector.



(a) Radial profiles at various stations downstream from helium injector.



(b) Axial profile along duct axis.

Figure 3. - Typical lateral turbulence intensity profiles. Stream velocity, 75 feet per second.

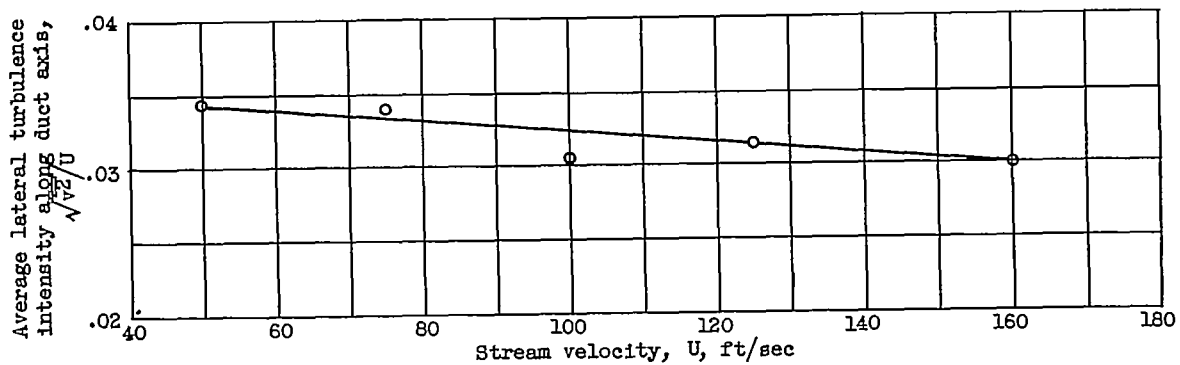
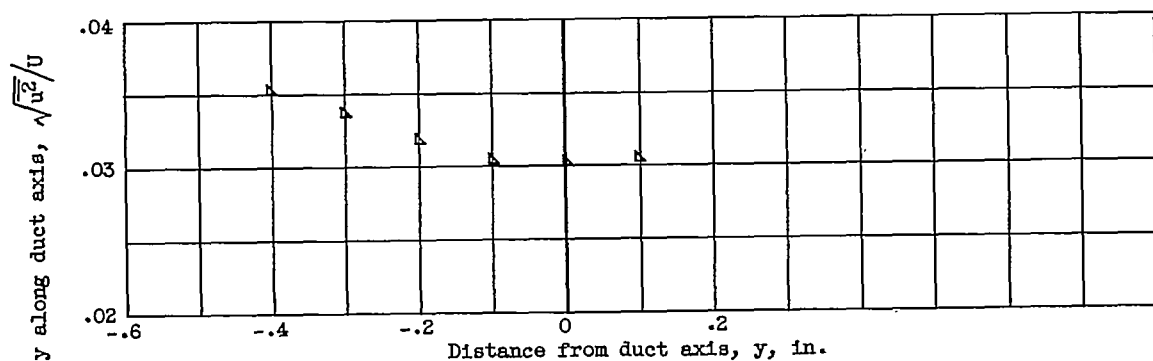
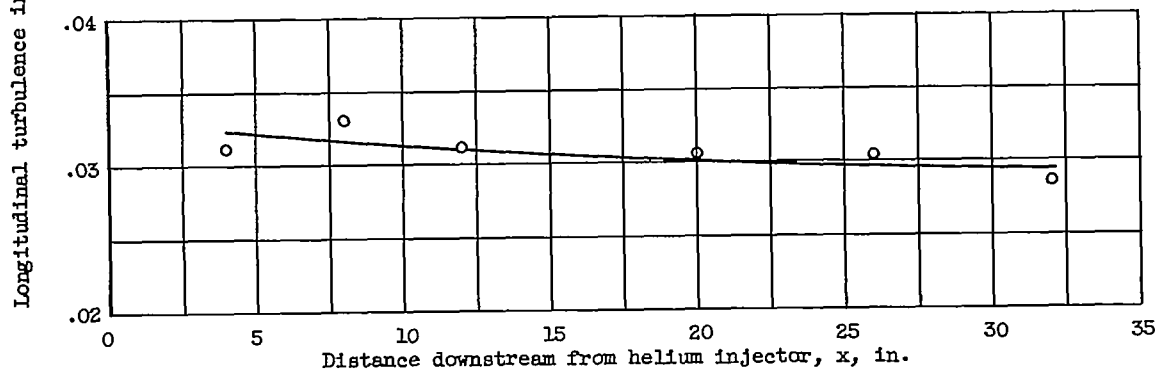


Figure 4. - Effect of stream velocity on lateral turbulence intensity along duct axis.

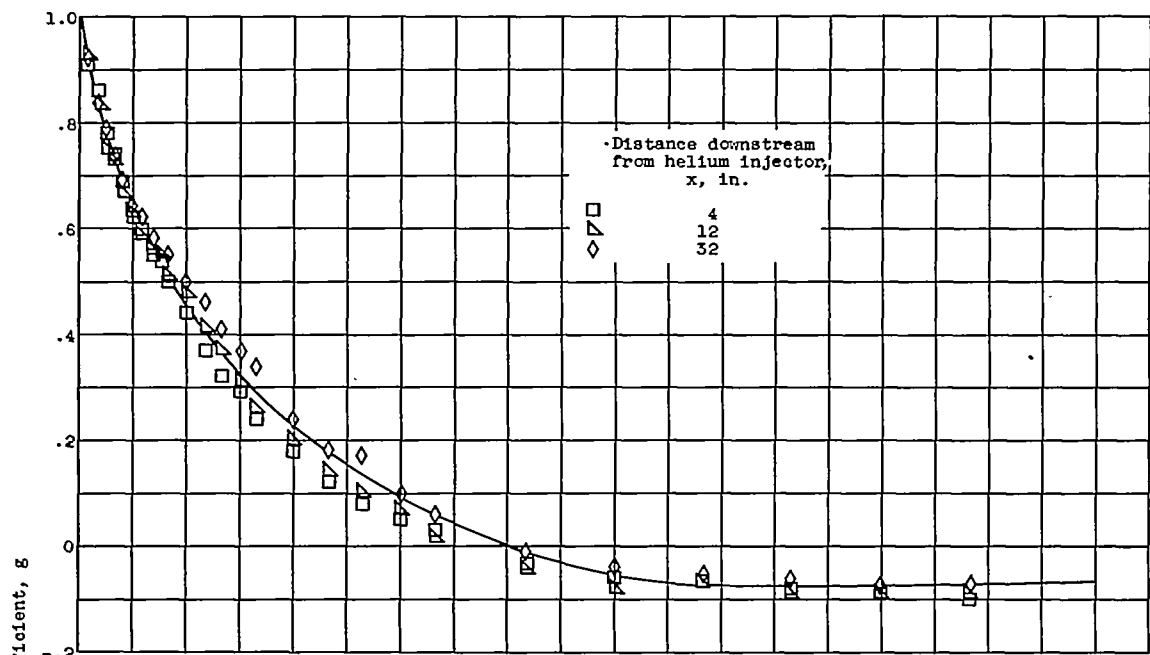


(a) Radial profile 12 inches from injector. Stream velocity, 50 feet per second.

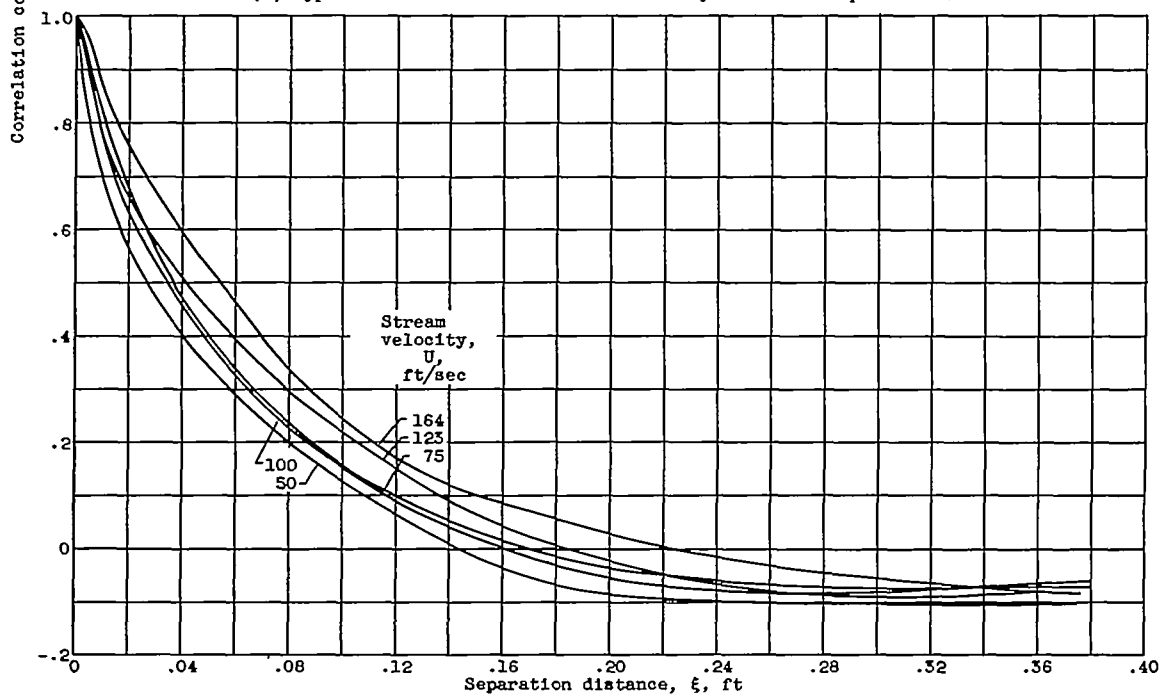


(b) Axial profile along duct axis. Stream velocity, 75 feet per second.

Figure 5. - Typical longitudinal turbulence intensity profiles.

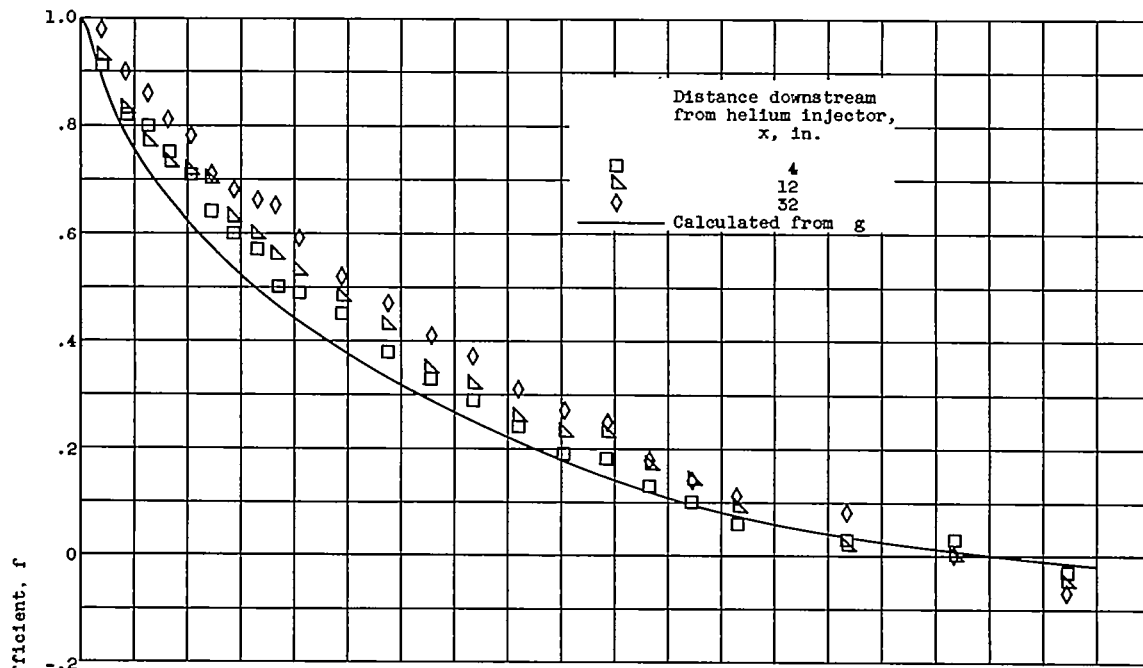


(a) Typical measurements at stream velocity of 100 feet per second.

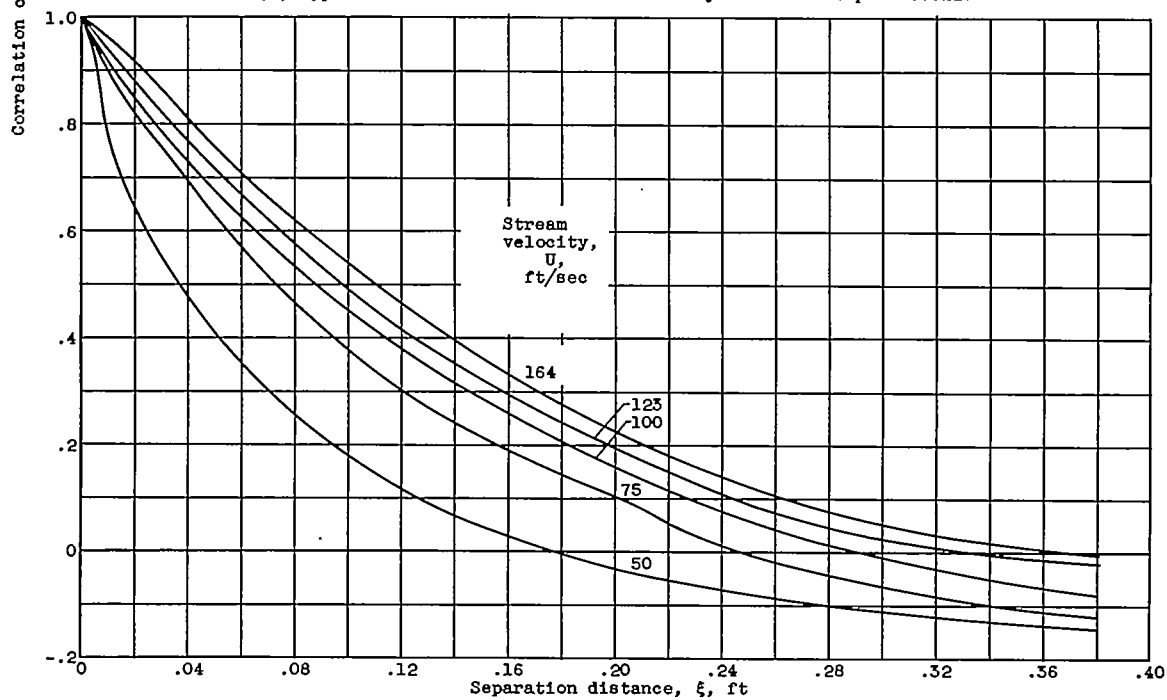


(b) Summary of radial measurements.

Figure 6. - Radial measurements of Eulerian correlation coefficient g along duct axis.



(a) Typical measurements at stream velocity of 123 feet per second.



(b) Summary of axial measurements.

Figure 7. - Axial measurements of Eulerian correlation coefficient f .

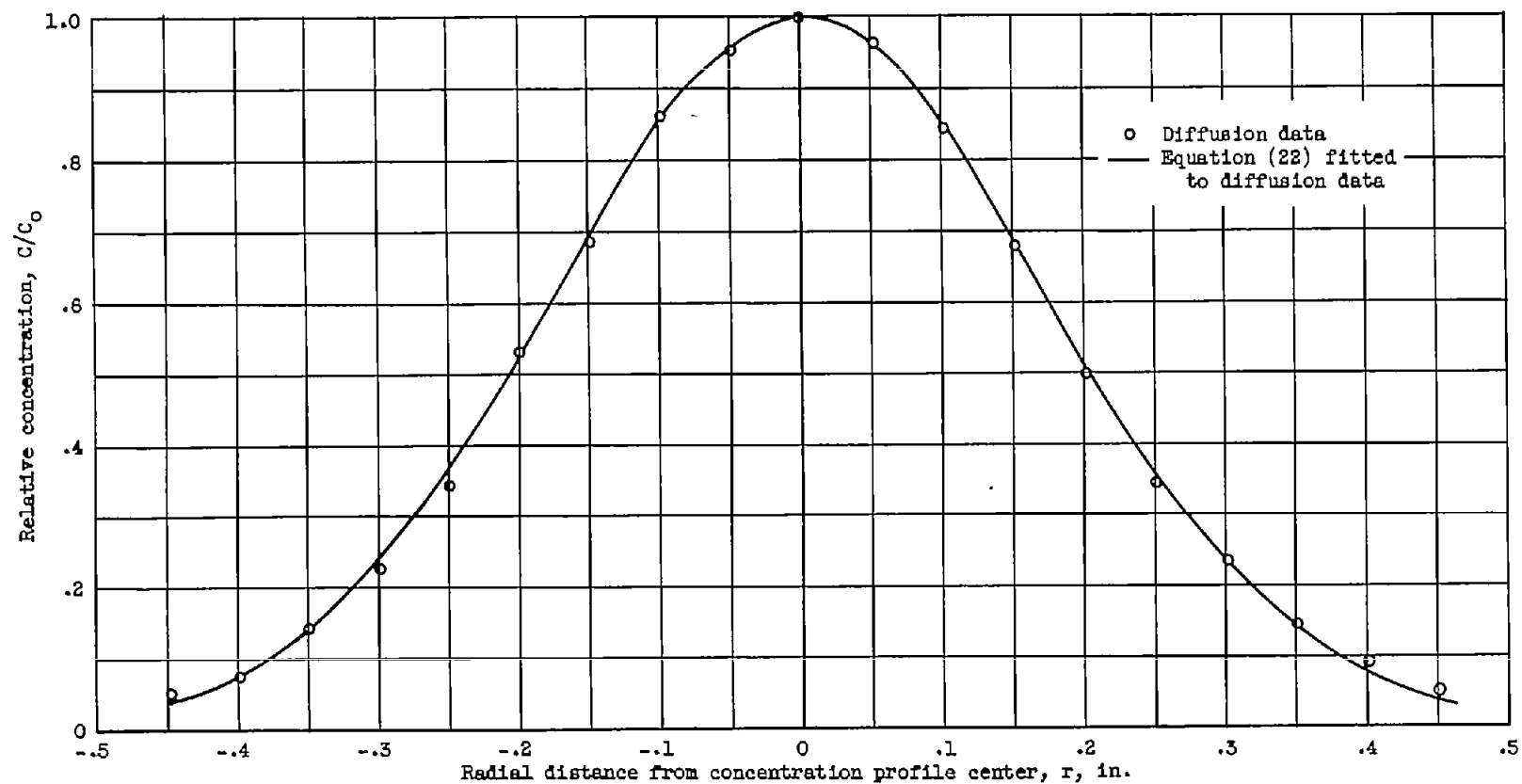


Figure 8. - Typical radial profile of helium concentration. Stream velocity, 50 feet per second; distance downstream from injector, 12 inches.

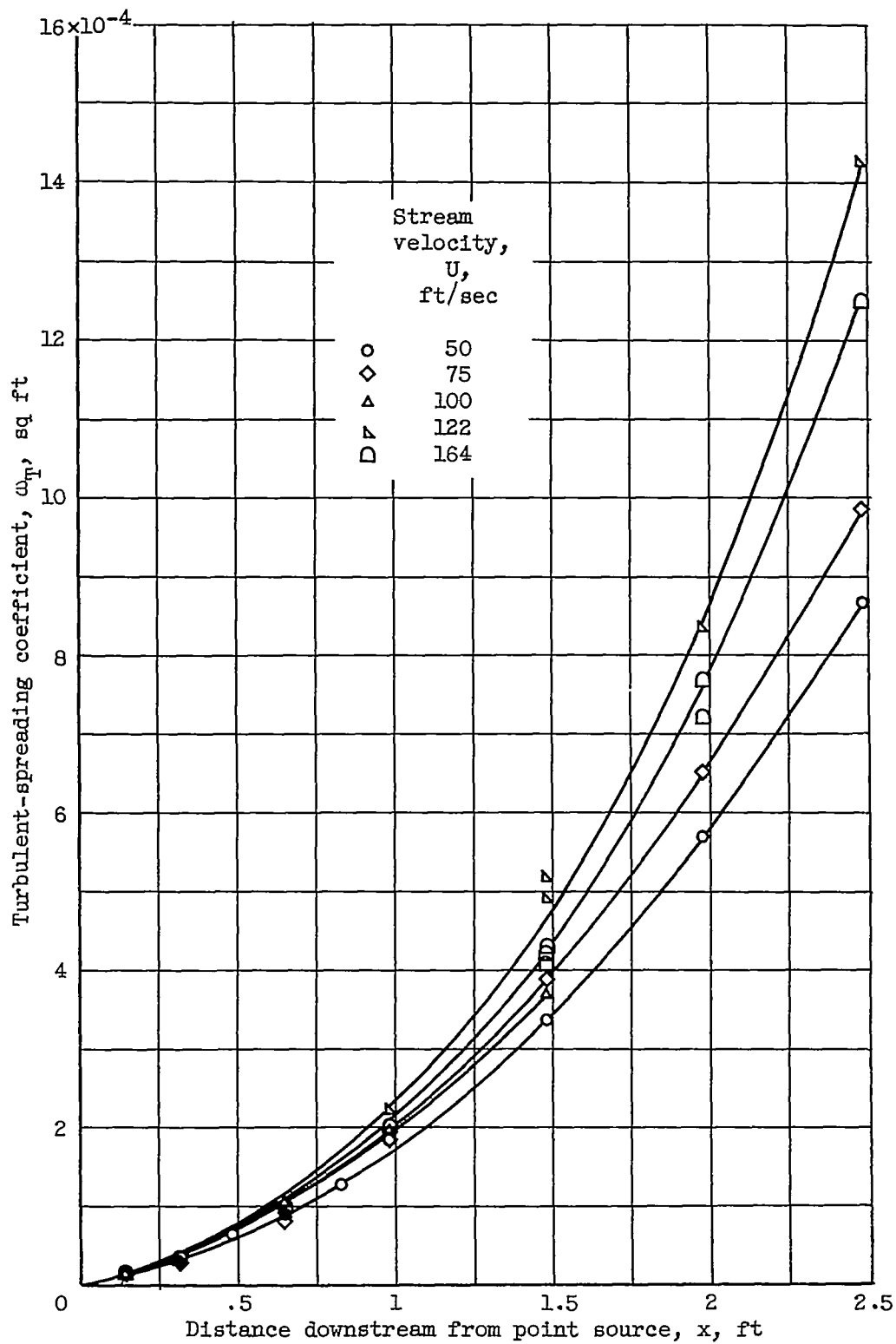


Figure 9. - Summary of turbulent-spreading-coefficient data obtained from helium concentration profiles.

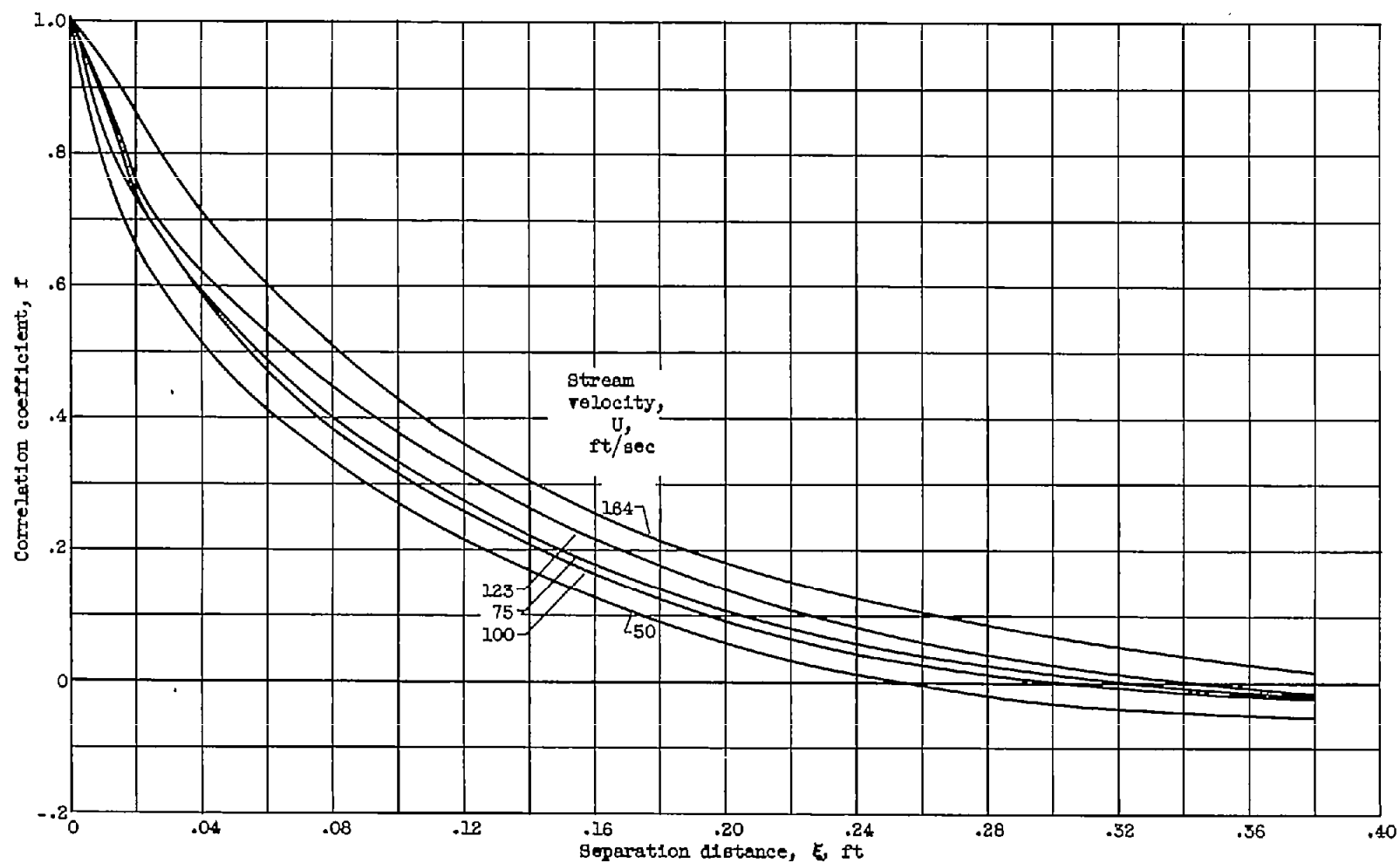


Figure 10. - Summary of correlation coefficient f calculated from measured correlation coefficient g .

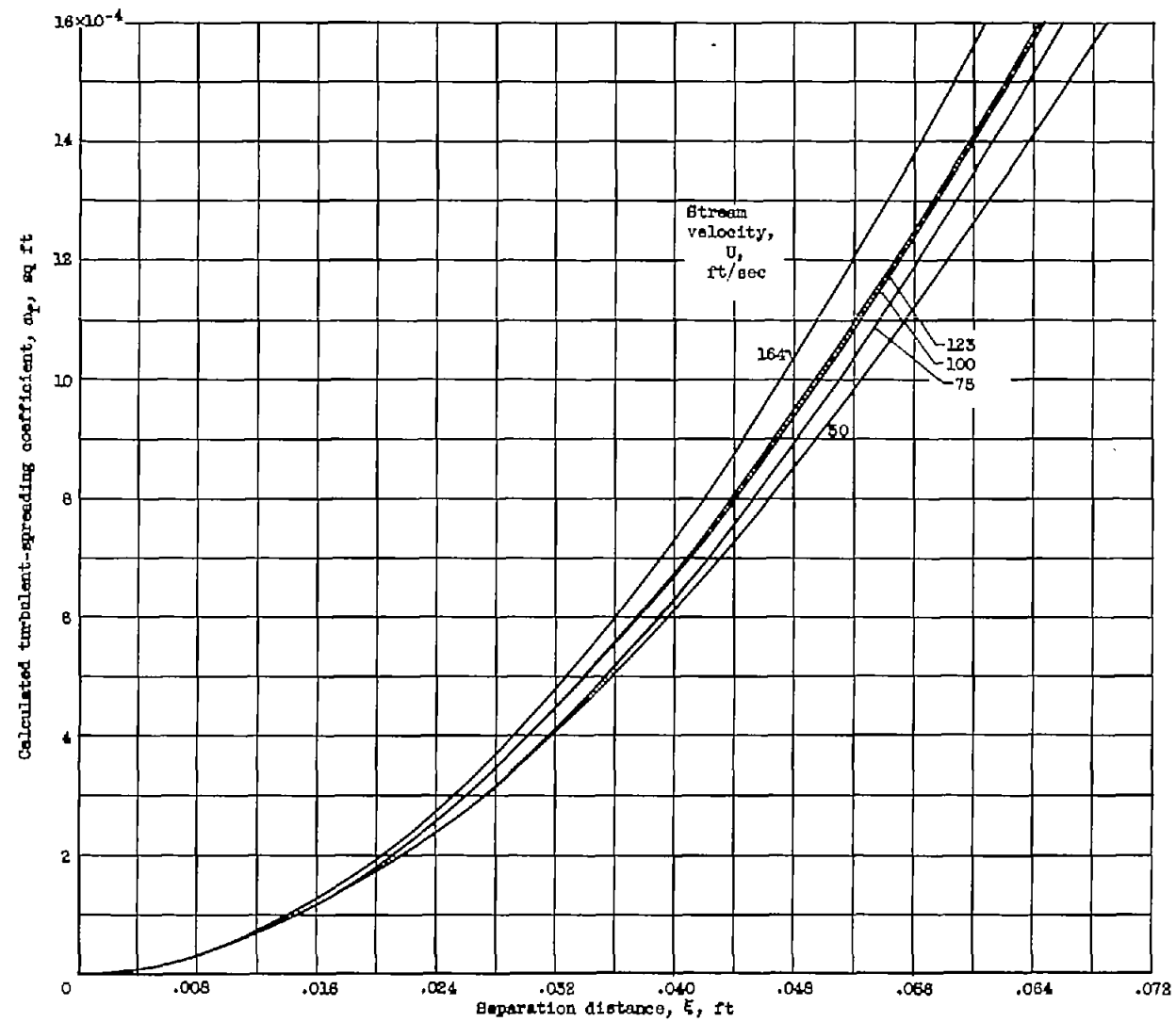


Figure 11. - Summary of turbulent-spreading coefficients calculated from Eulerian correlation coefficient f .

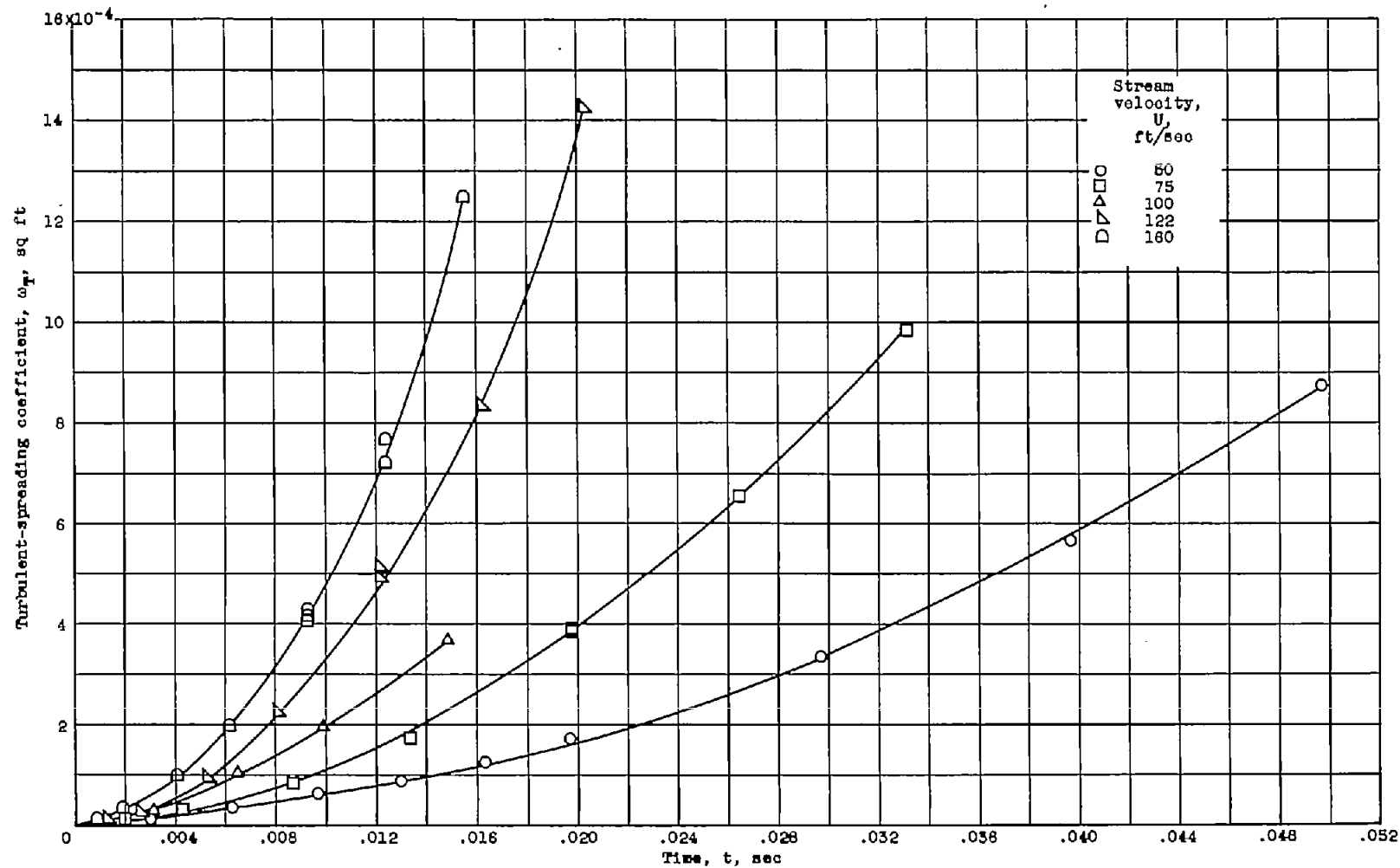


Figure 12. - Summary of time variation of turbulent-spreading coefficient measured by helium diffusion.

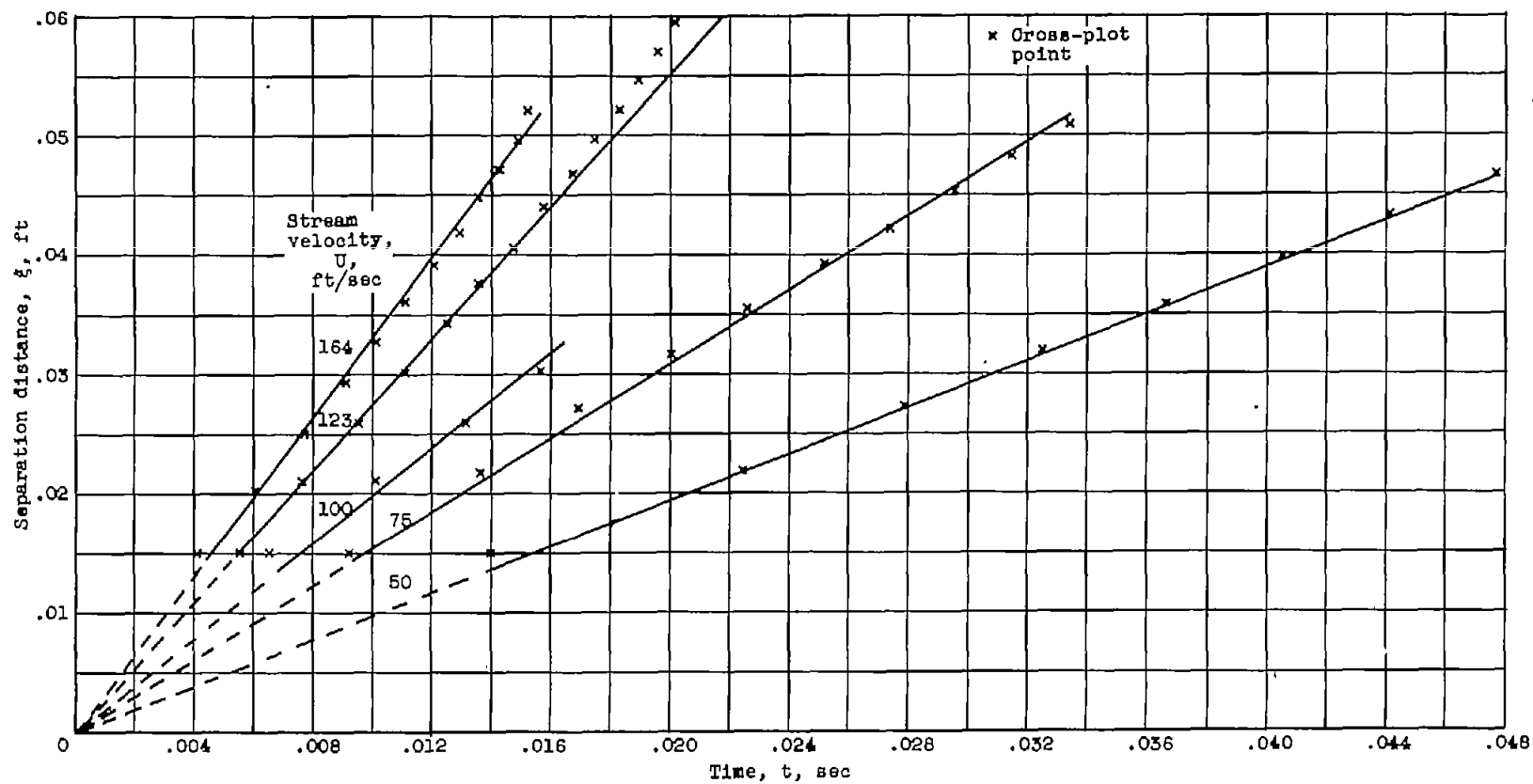


Figure 13. - Cross plot of figures 11 and 12 showing linear relation between slopes of Lagrangian and Eulerian correlation coefficients.

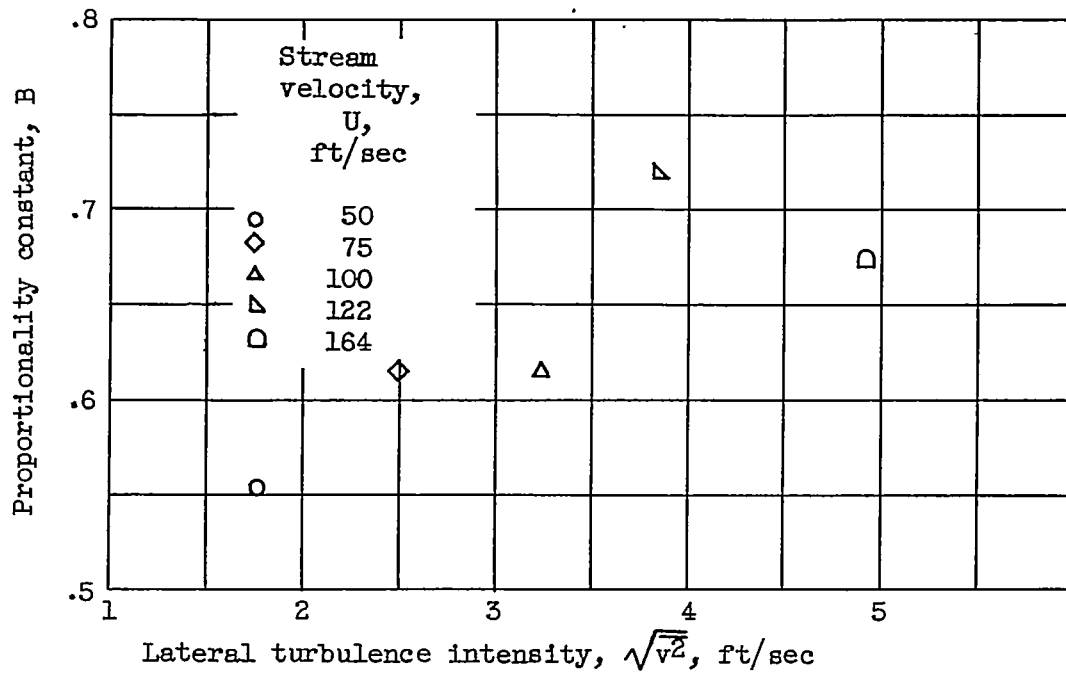


Figure 14. - Constant of proportionality in linear relation between shapes of Lagrangian and Eulerian correlation coefficients.

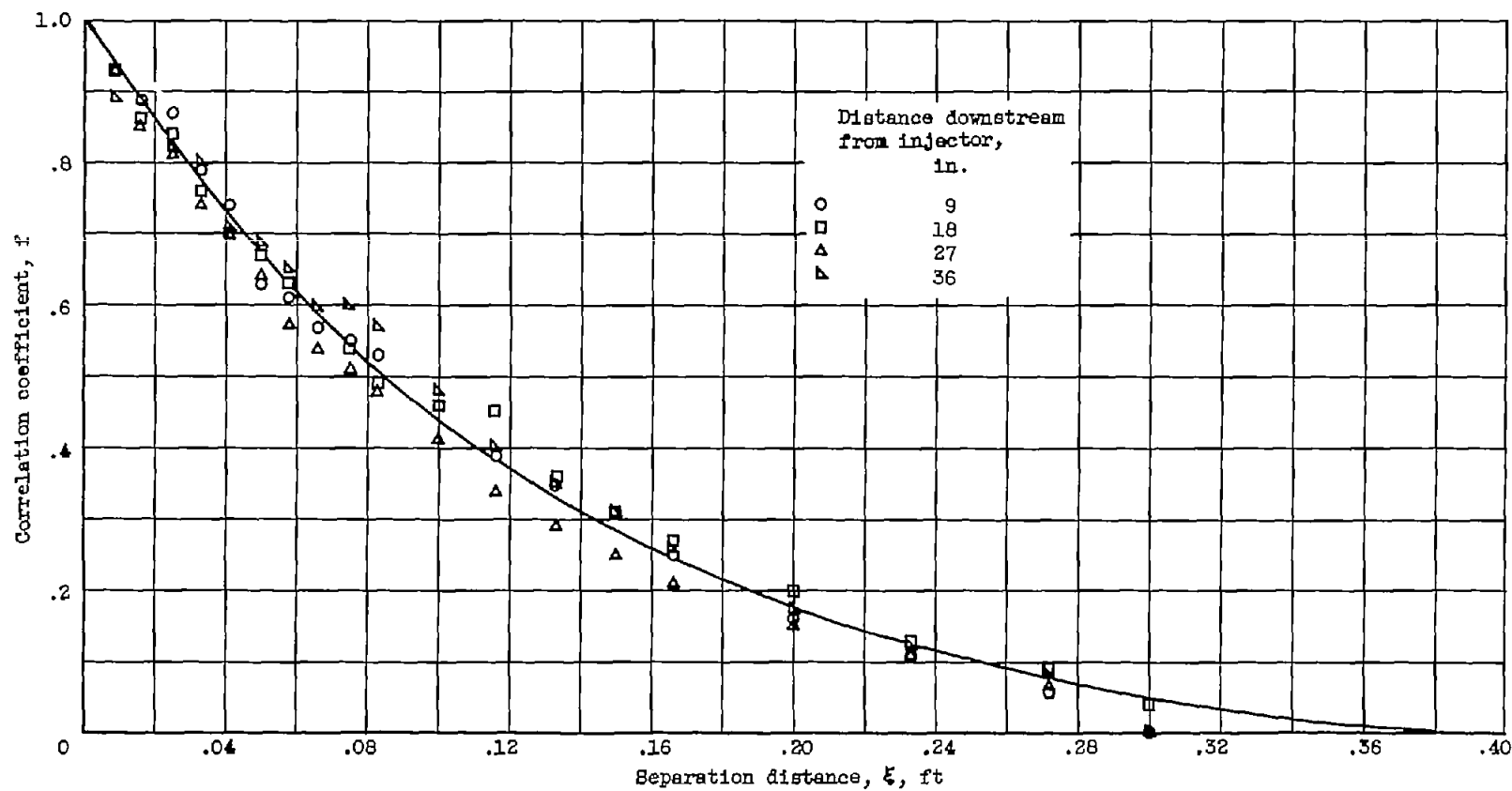
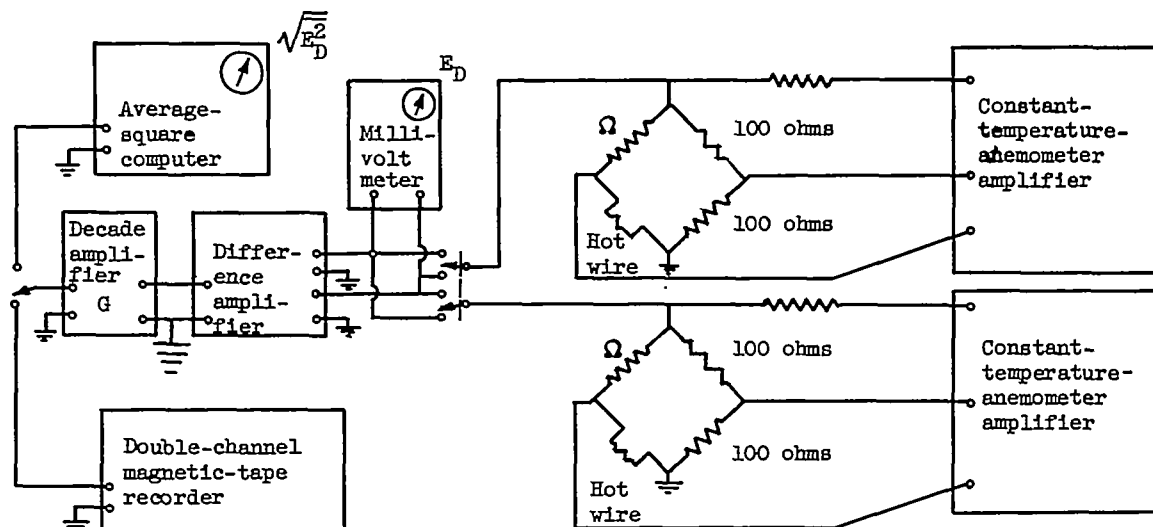
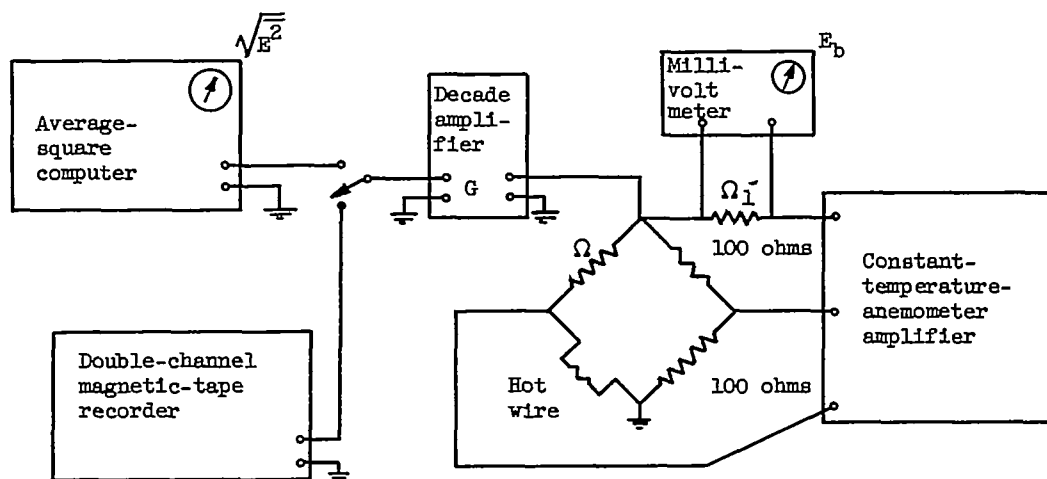


Figure 15. - Correlation coefficient f measured along axis of 6-inch-diameter duct. Stream velocity, 250 feet per second; static pressure, 1 atmosphere; static temperature, 235° F.



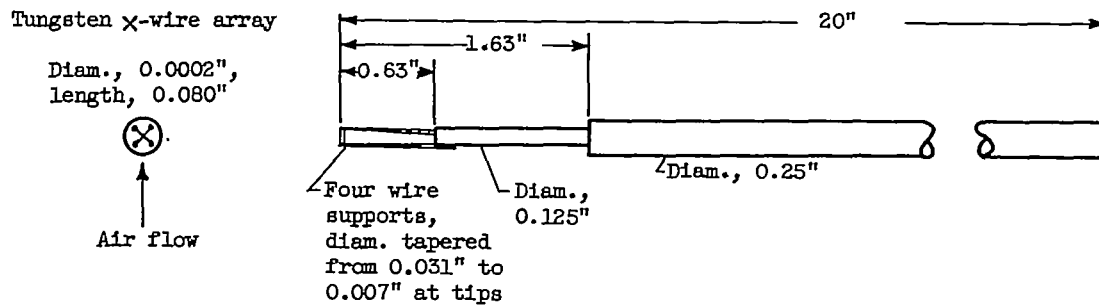
(a) Circuit used for lateral turbulence measurements.



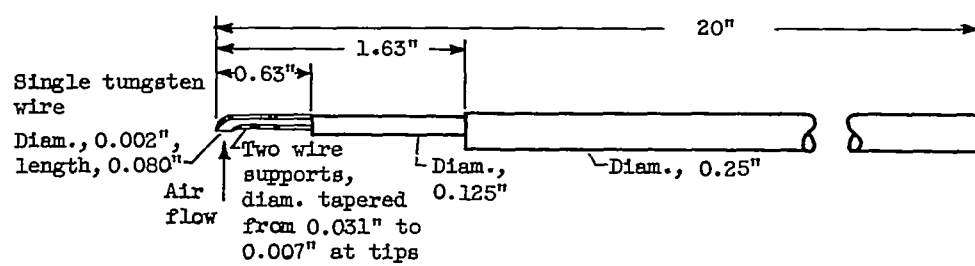
(b) Circuit used for longitudinal turbulence measurements.

Figure 16. - Hot-wire-anemometer circuits.

3781



(a) X-wire-anemometer probe.



(b) Single-wire-anemometer probe.

Figure 17. - Hot-wire-anemometer probes.

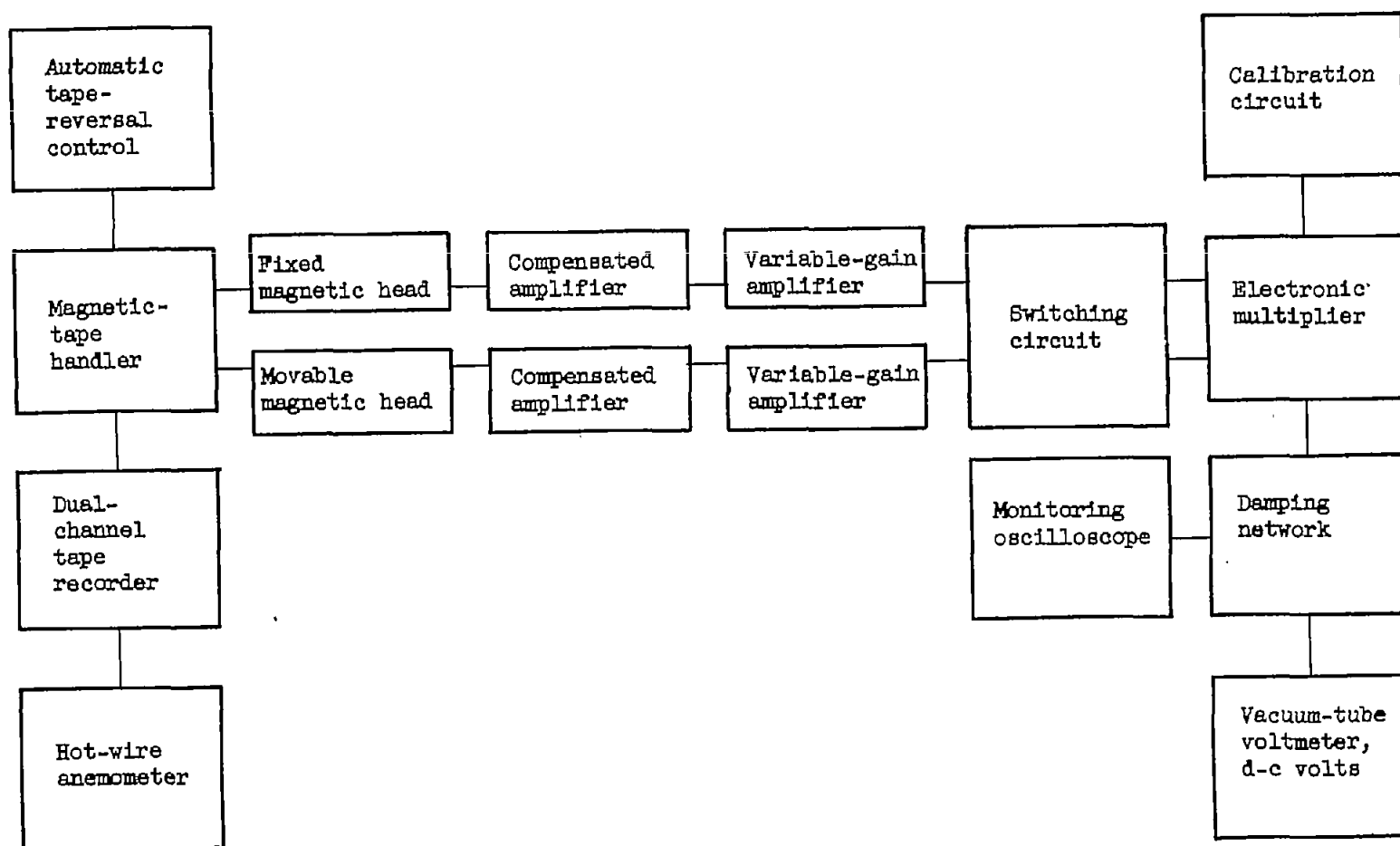


Figure 18. - Block diagram of correlation computer.